Order Number 1337960

Spray pyrolysis processing of yttrium-barium-copper-oxide and bismuth-strontium-calcium-copper-oxide superconducting thin films

Bania, William Roger, M.S.

The University of Arizona, 1989

U·M·I
300 N. Zeeb Rd.
Ann Arbor, MI 48106

SPRAY PYROLYSIS PROCESSING OF YTTRIUM-BARIUM-COPPER-OXIDE AND BISMUTH-STRONTIUM-CALCIUM-COPPER-OXIDE SUPERCONDUCTING THIN FILMS

by

William Roger Bania

A Thesis Submitted to the Faculty of the

DEPARTMENT OF MATERIALS SCIENCE AND ENGINEERING

In Partial Fulfillment of the Requirements

For the Degree of

MASTER OF SCIENCE

In the Graduate College

THE UNIVERSITY OF ARIZONA

1 9 8 9

STATEMENT BY THE AUTHOR

This thesis has been submitted in partial fulfillment of requirements for an advanced degree at the University of Arizona and is deposited in the university library to be made available to borrowers under rules of the library.

Brief quotations from this thesis are allowable without special permission, provided that accurate acknowledgement of source is made. Requests for permission for extended quotation from or reproduction of this manuscript in whole or in part may be granted by the head of the major department of the Dean of the Graduate College when in his or her judgment the proposed use of the material is in the interests of scholarship. In all other instances, however, permission must be obtained from the author.

SIGNED: William J. Brown

APPROVAL BY THE THESIS DIRECTOR

This thesis has been approved on the date shown below:

S. H. Risbud — 7-25-89

Subhash H. Risbud
Professor of Materials Science
and Engineering

Date

ACKNOWLEDGEMENTS

I wish to thank Professor Subhash H. Risbud, for his help and guidance throughout the course of this work. I would also like to thank Dr. Keating for allowing me to T.A. his classes and for reviewing my thesis. I would also like to thank Dr. Leavitt and Dr. McIntyre for performing RBS work on my samples.

I am indebted to the National Science Foundation for supporting this research by the Materials and Engineering Processing Program under Grant MSM-87171790.

I would also like to thank all the member's of Professor Risbud's research group for their help and friendship.

Finally I would like to thank my entire family, my parents, my grandparents, and my aunts and uncles, for their support and encouragement throughout my college years. Also I wish to thank Carla Covey, that special someone. I Love you woman.

TABLE OF CONTENTS

LIST OF ILLUSTRATIONS

Figure

LIST OF ILLUSTRATIONS--CONTINUED

LIST OF TABLES

ABSTRACT

The purpose of this investigation was to explore the processing parameters involved in the production of thin film superconductors by spray pyrolysis processing (SPP). The present study is an attempt to optimize the many parameters in SPP. The specific parameters studied were substrate temperature, carrier gas flow rate, substrate materials, solution stoichiometry, spray rate, concentration, starting materials, and substrate to nozzle distance. The effect of these parameters on film stoichiometry and the anticipated superconducting behavior were investigated at some length. Films were routinely produced in a spray chamber designed as a part of this research. Films were analyzed by Rutherford Backscattering Spectroscopy, X-Ray Diffraction, Scanning Electron Microscopy, and Meissner effect measurements.

CHAPTER I: INTRODUCTION

The discovery of the oxide ceramic superconductors by Bednorz and Muller has triggered vigorous worldwide activity in many research groups involved in processing and properties of these new supercondutors.[1] Superconductors have historically been metallic in nature and thus could be produced by standard metallurgical methods. The new ceramic superconductors present many interesting processing challenges because of their chemical and structural complexity.

Methods for bulk ceramic processing include sintering, hot isostatic pressing (HIPing), explosive compaction, extrusion, and melt texturing. Thin film techniques used include chemical vapor depositon, molecular beam epitaxial growth (MBE), plasma-assisted chemical vapor depositon, spin coating, and spray pyrolysis processing (SPP).

The need for developing a low cost method of preparation makes spray pyrolysis processing (SPP) an attractive method for producing ceramic oxide superconductors.

The purpose of this investigation was to explore the processing parameters involved in the production of thin film superconductors by spray pyrolysis processing (SPP). The present study is an attempt to optimize the many parameters in SPP. The specific parameters studied were substrate temperature, carrier gas flow rate, substrate materials, solution stoichiometry, spray rate, concentration, starting materials, and substrate to nozzle distance. The effect of these parameters on film stoichiometry and the anticipated superconducting behavior were investigated at some length.

Films were routinely produced in a spray chamber designed as a part of this research. Films were analyzed by Rutherford Backscattering Spectroscopy, X-Ray Diffraction, Scanning Electron Microscopy, and Meissner effect measurements.

CHAPTER II. LITERATURE SURVEY

II. A. SPRAY PYROLYSIS PROCESSING

SPP is a process in which a low molar concentration solution is sprayed onto a heated substrate. On the substrate the solution goes through an endothermic reaction (pyrolysis). The volatile by-products are evaporated and a crystallite or a cluster of crystallites is formed. A typical SPP set up is shown in Figure 1.

II. A. 1. HISTORY

SPP has its origins in the glass industry. It was originally used in the early 1900's for applying decorative and abrasion resistant coatings on glasses.[2] Mochel in the 1950's developed and patented several SPP methods for producing transparent conductive tin oxide films on glass.[3] Further development of this technique by Chamberlin and Skarman in the late sixties, produced sulfide and selenide films.[4] This research was prompted by the photovoltaic (PV) industry.

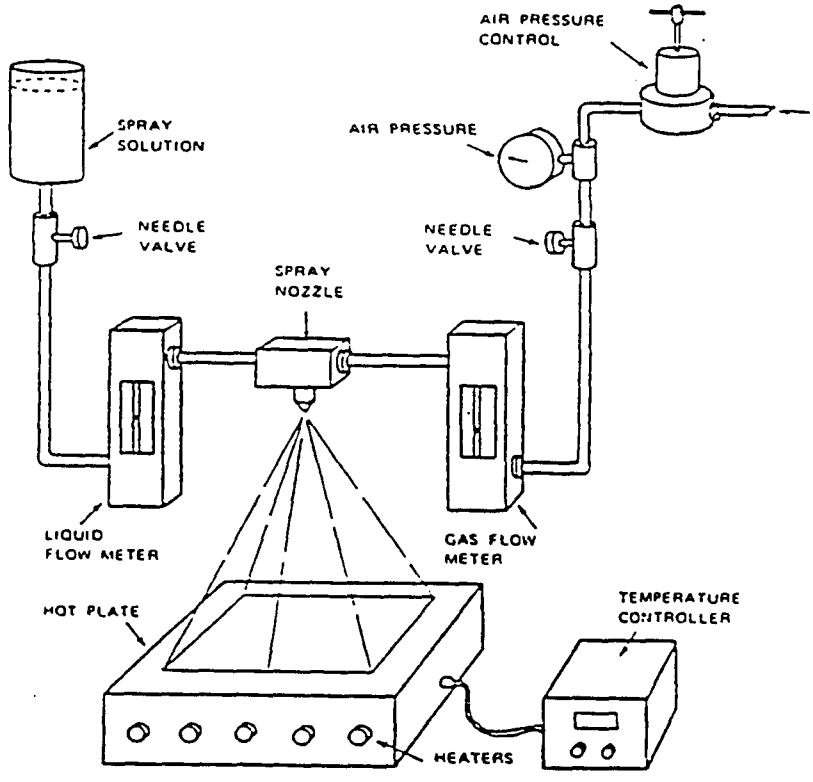

FIGURE 1: Typical Spray Pyrolysis Set-up. For this study the hot plate is enclosed in a lucite box.

In the PV industry, expense and efficiency are the two most important factors. In no other industry are these two factors more heavily scrutinized when developing a technique or a material for use. A ratio of efficiency to cost was thus developed to provide more insight into this delicate balance. Highly efficient (>20%) PV cells can be produced by MBE of gallium arsenide. However, the cost of producing these cells is quite high, and MBE cells cannot be mass produced easily. On the other hand, SPP PV cells can be produced relatively inexpensively.

A possible drawback of SPP is that the films produced are typically polycrystalline or amorphous. With the decreased crystalline perfection, as compared to single crystal films, the efficiency is generally lower. Efficiency of a solar cell is defined as the percentage of incident solar radiation is converted to electrical current. However, the smaller efficiency is outweighed by the low cost of deposition.

Currently, the most actively researched materials in SPP are $CuInS_2/CuInSe_2$, SnO_2, and CdS. Since this technique can cover a large area inexpensively, its cost effectiveness is unmatched by any other technique. It is important to

note that SPP is a more versatile and less expensive method than MBE, CVD, and evaporation. Since most of these methods require a high vacuum and very expensive processing equipment, they are not easily scaled up into large scale applications. Commercially, Cu_2S-CdS PV arrays of size 60 cm by 50 cm have been produced by Photon Power Company, by a continuous roller spray deposition process.

More recently, SPP has been used to apply superconductors on a variety of substrates.[5,6] These films are easily produced, however, they are difficult to reproduce without careful optimization of the processing parameters.

II. A. 2. PROCESSING PARAMETERS

Processing parameters for SPP include the following: ambient temperature, substrate temperature, substrate material, carrier gas flow rate, nozzle to substrate distance, solution concentration, solution flow rate, solution chemistry, and if a continuous process is used, substrate motion.

These can be categorized into several primary areas: temperature effects, solution conditions (including starting materials), dynamics of the spray, and substrate effects.[7] Their effects on films are discussed below.

II. A. 2. a. TEMPERATURE EFFECTS

Temperature is probably the most important parameter to control. It can have a dramatic effect on the properties and the structure of the films produced. The first item to consider is the substrate heater.

There are several ways to heat the substrate. The substrate heater is typically a metal block heated with either cartridge heaters, a liquid metal bath or infrared lamps. An advantage of liquid metal baths over the other techniques is, it can provide a better thermal contact between the substrate and the hot liquid metal surface. Even the most perfect solid to solid surfaces are in contact at less than 1% of the surface area.[8] Heating by radiant heat sources can be used if there is a problem with corrosive vapors in contact with liquid metals.[9] Several investigators have been able to control the temperature to within $\pm$5°C.[10,11] Obtaining a hot substrate is not as much

of a problem as measuring the surface temperature of the substrate. During spraying the substrate is constantly cooled by droplets hitting the surface. Infrared pyrometers have been used, but have shown a temperature difference of 50°C between a molten tin oxide bath and the substrate surface.[12]

The use of conventional thermocouples placed at or near the surface of the substrate is a currently accepted method of temperature measurement.

The effects of temperature on the structure of films can best be observed in the $CuInS_2$ family of films. At 225°C, films produced have the sphalerite structure, whereas at 300°C, films produced can have either the sphalerite structure or the chalcopyrite structure.[13]

Another well characterized system is the CdS family. Films produced by SPP are found to contain both the hexagonal and cubic structures. The ratio of these two strucutres has been determined to be a direct function of the substrate temperature.[14] Between 375° and 460°C, hexagonal structures predominate up to >90%. Temperatures greater than 460°C produced a rapidly decreasing amount of

the hexagonal structure and an increase in the amount of the cubic structure.

II. A. 2. b. SOLUTION CONDITIONS

Starting materials for SPP are chosen on their ability to dissolve in aqueous solutions. Chlorides, nitrates, oxides and organic compounds can all be used, with differing effects on the final film. To produce good quality $CuInSe_2$ films, and thus good quality devices, $CuCl_2$ and $Cu(C_2H_3O_2)_2$ can both be used. However, when $CuCl_2$ is used, the acidity of the solution must be neutralized to a pH of 3, in order to form the preferred chalcopyrite structure.[13] Films sprayed at <225°C, regardless of the pH, have the sphalerite structure.

For oxide deposition there are several guidelines to choosing the starting chemicals. The starting chemicals should be stable at room temperature, not be easily oxidized and decompose at temperatures <500°C.[15]

With multi-component systems an important aspect to consider is the solubility limit of the cation species, when other cations are present. Eh-pH diagrams are used in

determining the regions of stability for the individual cations. Eh or oxidation potential, is a thermodynamically derived property, which has units of electron volts. pH is the negative log of the hydrogen ion concentration. Figure 2 shows an Eh-pH diagram for copper in water. Note there are several lines between Cu^{2+} and $Cu(OH)_2$. The numbers -2, -4, and -6 refer to the total cation molarity. (ie -2 = 10^{-2} M) With the copper system, as the total molarity of cations increases, the area of stability of the Cu^{2+} cations decreases.

The solution pH, as with the substrate temperature, has the effect of changing the structure that is produced. When 90% of the acid is neutralized when using $CuCl_2$ to produce $CuInS_2$ films, the chalcopyrite structure is dominant.[13]

Table I shows the variety of starting materials and solutions that can be used by SPP.

II. A. 2. c. SPP SPRAY DYNAMICS

An important piece of the spraying apparatus is the spray nozzle. There are a variety of spray nozzles that can be used, ranging from a pipette to a commercially

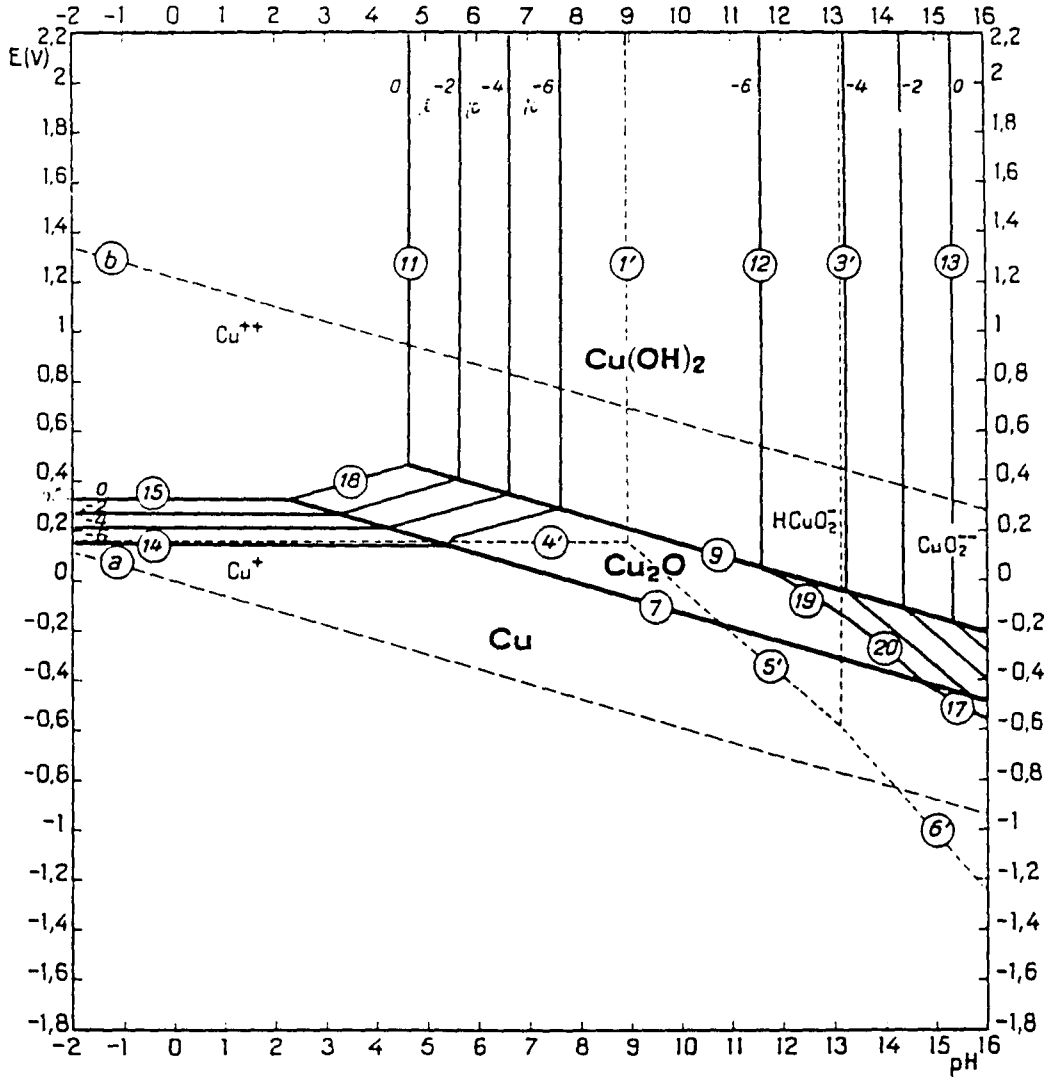

FIGURE 2: Eh-pH equilibrium diagram for the Copper-water system at 25°C. (Ref.50)

TABLE I: SPP films and Their Starting Materials and Solvents.

Film	Starting Materials	Solvent
SnO_2	$SnCl_4$	H_2O + HCl H_2O + alcohol
	$SnCl_2$	Ethanol
	$SnBr_4$	HBr
	$(NH_4)_2SnCl_6$	H_2O
	$(CH_3COO)_2SnCl_2$	Ethyl acetate
In_2O_3	$InCl_3$ or $InCl_2$	Butyl acetate, or butanol
	$InCl_3$	Methanol-water
ITO	$InCl_3$, $SnCl_3$	Methanol-water, ethanol-water
Cu_2S	$Cu(CH_3COO)_2$ + thiourea	Water
PbS	$Pb(CH_3COO)_2$, $PbCl_2$ $Pb(NO_3)_2$ + thiourea	Water
PbO	$PbCl_2$	Water
Cr_2O_3	Cr acetylacetonate	Butanol
Fe_2O_3	Fe acetylacetonate	Butanol
V_2O_3	Canadium acetylacetonate	Butanol
$CuInSe_2$	$InCl_3$, CuCl, N, N-dimethylselenourea	H_2O
$CuInS_2$	$InCl_3$, CuCl, or $CuCl_2$, N, N-dimethylthiourea	H_2O
$CuGaS_2$	$InCl_3$, CuCl, or $CuCl_2$, N, N-dimethylthiourea	H_2O

available spray nozzle to an ultrasonic atomizer. Figure 3 shows four different nozzles which that been used. It is important to note that, the finer the droplet diameter, the better are the chances for complete pyrolysis. With these spray apparati, there is a potential for the spray nozzle to become partially clogged and/or eroded. Therefore ultrasonic atomizers are becoming the state of the art spray nozzle for SPP.[15,16,17] They do not have a nozzle that the solution is sprayed from, thus eliminating clogging and erosion. An ultrasonic atomizer produces a very fine mist, which can be directed at a substrate.

II. A. 2. d. SUBSTRATE EFFECTS

Films grown using a low molar solution concentration (<0.01M) and at a slow rate produce epitaxial films. However, due to the long spray times and slight variations in substrate temperature, epitaxial films are difficult to produce. Most films produced, therefore, are either polycrystalline or amorphous.

The choice of substrate materials has a direct effect upon the quality and structure of the film. Diffusion of an element or elements from the film into the substrate,

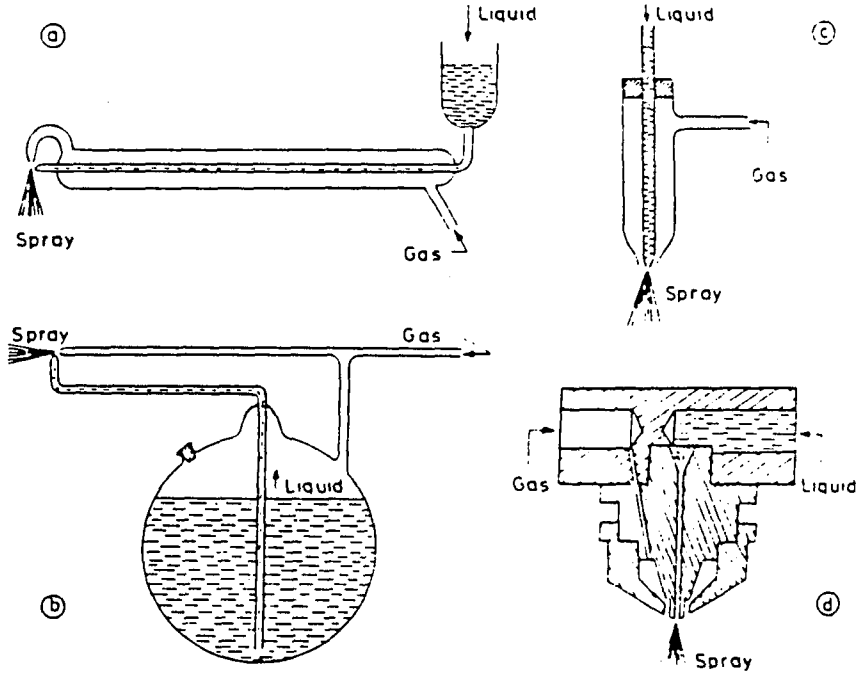

FIGURE 3: Nozzles currently used in Spray Pyrolysis Processing. Nozzle (d) is a commercially available and is the nozzle used in this study.

produces an unwanted reaction zone, which has a detrimental effect on the desired properties of the films. Chemical reactivity between the film and the substrate is an issue which has been investigated by many researchers. Barrier layers have been used to prevent such a reaction zone from occurring. For the $Y_1Ba_2Cu_3O_7$ films produced on single crystal yttria stabilized zirconia, yttria barrier layers are used.[18,19]

II. 3. SPP MECHANISMS

There are four different processes which can describe the reactions which occur at the substrate. These are shown schematically in Figure 4. In process A, the droplet hits the substrate, still in the liquid form. The droplet either impinges on the substrate and the solvent evaporates, leaving behind the desired materials, or it skips off the substrate, much like rain drops on a newly waxed car. In process B, evaporation of the solvent occurs before the droplet hits the substrate. The dry solid then impinges on the substrate or is blown off by the carrier gas. If it impinges, further decomposition or oxidation can then occur. Process C has the solid from process B melting and vaporizing. The vapor then diffuses to the substrate and

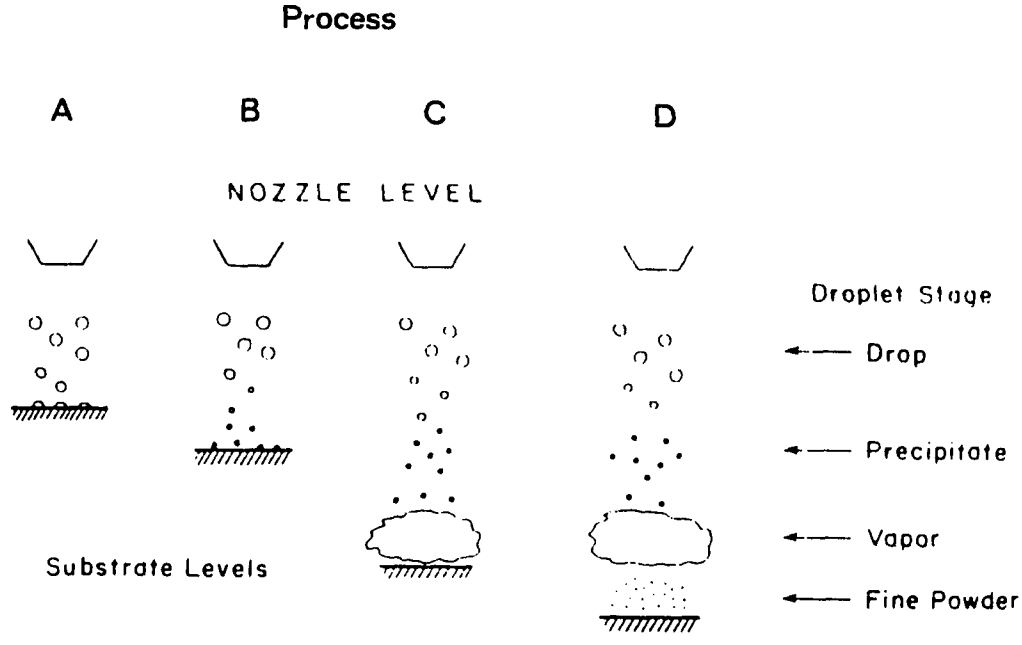

FIGURE 4: Four processes which can occur when depositing films via SPP. Process A is the most common process when producing SPP films.

deposits. This is considered to be a true chemical vapor deposition. Process D carries process C even further. The vapor is further heated to become fine particles, which impinge on the substrate.

Process A is the process which occurs in a majority of SPP set-ups.[8] With this process it is important to obtain the maximum number of droplets having the same volume and momentum to hit the substrate. After the droplet hits the substrate it spreads out into a disk.[20,21] The solvent evaporates leaving behind the solid disk. This process is repeated with each succeeding droplet, until processing is completed. The film will therefore consist of interspersed disks.[22] It has been calculated for a solution flow rate of 4 ml/min on an area of 80 cm^2, that a droplet hits the same area of the substrate once every 30 ms, or 33 drops per second.[23] The solid therefore does not have time to undergo much grain growth, consequently, most SPP films are fine grained. Further heat treatment has been used to produce larger grains.

II. B. SUPERCONDUCTIVITY

Superconductivity is probably one of the most startling discoveries of the 20th century. In the mid 1950's the transistor became reality, thus the era of microelectronics was born. In the 1970's integrated circuits became reality. And in the late 1970's early 1980's it was possible to put enough circuity on to a single chip that desktop computers have become as commonplace as the family vehicle. Then, in January 1986, a startling discovery by two Swiss IBM employees, Bednorz and Muller, may have changed the world forever. They discovered a superconducting compound with a transition temperature greater than 30 K. This began one of the world's largest scientific investigations of this century. 30 K may not sound especially high, considering the previous record was only 6.5 K lower than this record. But this was a La-Ba-Sr-O compound, a ceramic material. This provided a new source for researchers to look for superconducting compounds. Ceramics are generally considered excellent electrical insulators. But when this compound is cooled to 30 K, its resistance goes to zero.

II. B. 1. WHAT IS SUPERCONDUCTIVITY

To understand all the hubbub and fury of research recently in superconductivity, one must understand the

importance of superconductivity. What is superconductivity? Superconductivity is a physical state that allows the flow of electricity without any resistance. This state is dependent upon the critical temperature (T_c), below which there is zero resistance to current flow. The quality of a superconductor is based upon three characteristics: (1) the ability to carry dc electrical current without any losses, (2) the ability to repel magnetic fields, dependent upon its critical magnetic field, and, (3) quantity of electrical current it is able to carry, commonly called critical current density (amps/cm^2). These properties can best be described by how they can be used in applications.

II. B. 2. USES FOR SUPERCONDUCTORS

What can these superconductors be used for? Superconductors are currently used in a variety of applications, in particular the medical imaging field. Magnetic resonance imaging is accomplished by using superconducting magnets to produce strong magnetic fields which can give doctors a three dimensional image of a person's body, without surgery. The image is produced by a difference in the chemical compositions of the various tissue types in the human body.

Another use for superconductors, is as a SQUID, Superconducting Quantum Interference Device. A SQUID can detect the most minute electromagnetic signals, as low as one ten-billionth of the earth's magnetic field. With this sensitivity it can be used to explore for oil deposits, undersea communications, nondestructive evaluation, and detecting neural impulses in the brain. A SQUID is composed of two Josephson junctions. A Josephson junction is a superconducting switch, which can switch with a switching time of as low as six pico seconds. This is ten times faster than a semiconductor switch.

There are many other applications for superconductors, Table II is a compilation of various uses for them.

II. B. 3. HISTORY OF SUPERCONDUCTORS

Mercury was the world's first superconducting material. In 1911, H. Kammerlingh Onnes discovered that upon cooling mercury to below 4.2 K it became superconducting.[24] Soon after this discovery, most pure metals were found to be superconducting. Appendix I contains a representative list of metals and their superconducting transition temperatures.

TABLE II: Possible Uses for Superconductors

Medicine	Magnetic Resonance Imaging
Computers	4 bit Microprocessor would run at 770 MHz
Sensors	SQUIDS
Antennas	Size would only need to be 5% or conventional antennas
Magnetic Refrigeration	Magnetic heat pumps
Power Transformers	Increase in power
Motor-Generator Sets	Saves weight and lower fuel consumption
Superconducting Ships	Japanese have built one that runs at 60mph
Bearings	Contactless bearings
3-D Flux Sensors	NDE for steel in concrete
Radiation Detectors	Far infra red detectors
Transmission Lines	Can carry 3 times more than copper wire
Particle Accelerators	Superconducting Super collider
Magnetic Levitation	Repulsion of magnetic fields
Magnetic Storage Devices	Huge Superconducting coils buried in the ground for storage of electricity
Magnetic Fusion Reactors	Fusion
Magnetohydrodynamic Systems	Produces electricity
Electromagnetic Launchers	
Magnetic Separation	
Crystal Growth	

Scientists in the superconducting society heralded new materials with a one or two degree increase in the transition temperature as a major breakthrough. Before 1986, the transistion temperature rose approximately 0.4°C/year to 23.5°C (Figure 5 and Appendix II). Then Bednorz and Muller discovered a 30 K superconducting material (La-Ba-Cu-O) in January 1986, which surpassed the old transistion temperature record by 6.5 K.

Within months after their discovery, many research groups around the world were reproducing this incredible achievement. [25,26,27] Researchers tried many different methods of producing this compound. However, processing would not be the key to raising the transition temperature, substitution would be. The logical step was to substitute other elements. Initially, strontium was replaced for barium and this was found to raise the transition temperature by five degrees to 40 K.[28,29,30] Practically every element on the elemental chart was tried in hopes of raising the transition temperature. Finally in April of 1986, Chu and Wu's groups made a startling discovery, using yttrium, barium, and copper in the following ratio, 1:2:3, a transition temperature between 90-100 K was achieved.[31] Within days, groups from around the world were verifying

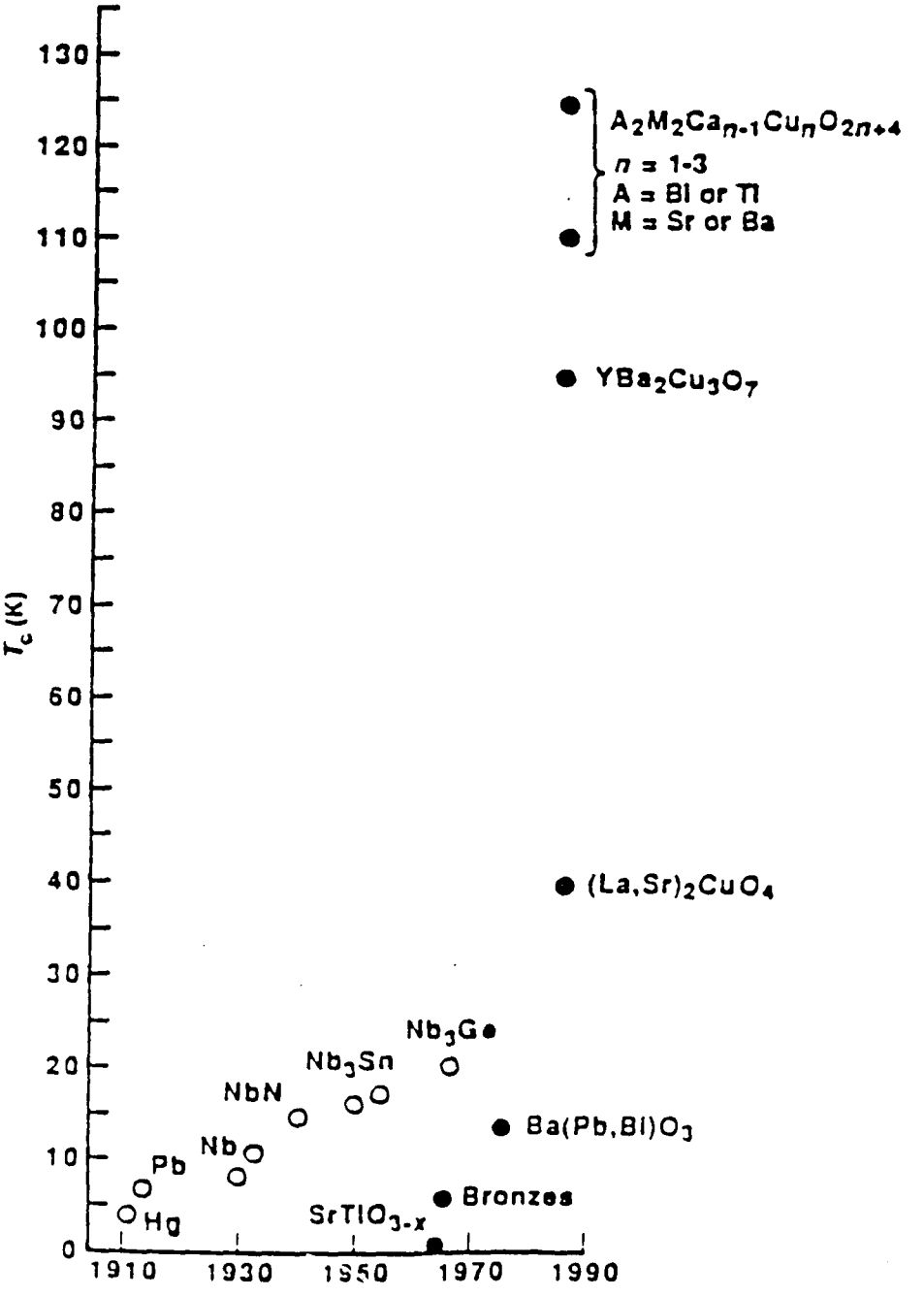

FIGURE 5: Highest T_c vs. date for superconductors. If a time line were drawn through the Niobium compounds, it can be seen that it would have taken 1000 years to achieve a 95 K superconductor.

this discovery.[32,33,34] This is the first time a transition temperature greater than the boiling point of liquid nitrogen (77 K) had ever been achieved. Previous superconductors still required liquid helium to cool them. With this discovery liquid nitrogen could now be used, a potential for savings was found. Liquid helium costs about $10 a liter, compared with $1 a liter for liquid nitrogen. This in itself was a major breakthrough.

In January and February of 1988, another new system of superconductors was discovered. This system involved the following two families, BiSrCaCuO and TlBaCaCuO.[35,36,37,38,39] These were announced in the Superconductivity News Letter and at the Interlaken meeting in Interlaken, Switzerland in February of that year.[40,41] The transition temperatures of these materials was in the range of 80-120 K.

Thus far superconductors with transition temperatures >77 K have had copper oxide planes. There is, however, a compound that superconducts with no copper present. It is an oxide composed of barium, bismuth, and lead.[42,43,44] In this compound, bismuth has three valence states, +3, +4, and +5. This is very similar to the Y-Ba-Cu-O compounds in that copper has two valence states present in this

superconductor, +2 and +3. The mixed valence states of the cations was the key to what Bednorz and Muller were looking for, when they discovered their superconductor.

There are three individual phases in the Bi-Ca-Cu-Sr-O system which have been identified. Table 3 shows the transition temperatures and compositions for several of the superconductors in this system. With such a large variety of compositional differences, multiple phases are typically produced in thin films and bulk samples.

II. B. 4. PROCESSING PROBLEMS OF HIGH Tc SUPERCONDUCTORS

There are several problems with both the Y-Ba-Cu-O and Bi-Ca-Cu-Sr-O superconductors. First, sintering of these materials is crucial. Since superconductivity is the ability to pass current through a material without any resistance to flow, grain boundaries become an issue. Large single crystals would be ideal, however, since the $Y_1Ba_2Cu_3O_7$ compound melts incongruently (Figure 6), single crystals cannot be grown by the Czorchalski method. Single crystals have been produced by flux growth and skull methods, which involves batching the materials in a crucible, melting, and then very slowly cool the melt for

TABLE III: Represenative list of known superconductors in the $(AO)_mM_2Ca_{n-1}Cu_nO_{2n+2}$ phases. NSC stands for non-superconducting.

Compound	T_c(K)	*n*	*m*
$TlBa_2YCu_2O_7$	NSC	2	1
$TlBa_2CuO_5$	NSC	1	1
$TlBa_2CaCu_2O_7$	90	2	1
$TlBa_2Ca_2Cu_3O_9$	110	3	1
$TlBa_2Ca_3Cu_4O_{11}$	122	4	1
$(Tl, Bi)Sr_2CuO_5$	50	1	1
$(Tl, Bi)Sr_2CaCu_2O_7$	90	2	1
$(Tl, Pb)Sr_2CaCu_2O_7$	90	2	1
$(Tl, Pb)Sr_2Ca_2Cu_3O_9$	122	3	1
$Tl_2Ba_2CuO_6$	90	1	2
$Tl_2Ba_2CaCu_2O_8$	110	2	2
$Tl_2Ba_2Ca_2Cu_3O_{10}$	122	3	2
$Tl_2Ba_2Ca_3Cu_4O_{10}$	119	4	2
$Bi_2Sr_2CuO_6$	12	1	2
$Bi_2Sr_2CaCu_2O_8$	90	2	2
$Bi_2Sr_2Ca_2Cu_3O_{10}$	110	3	2
$Bi_2Sr_2Ca_3Cu_4O_{12}$	90	4	2
$Bi_2Sr_2YCu_2O_8$	NSC	2	2

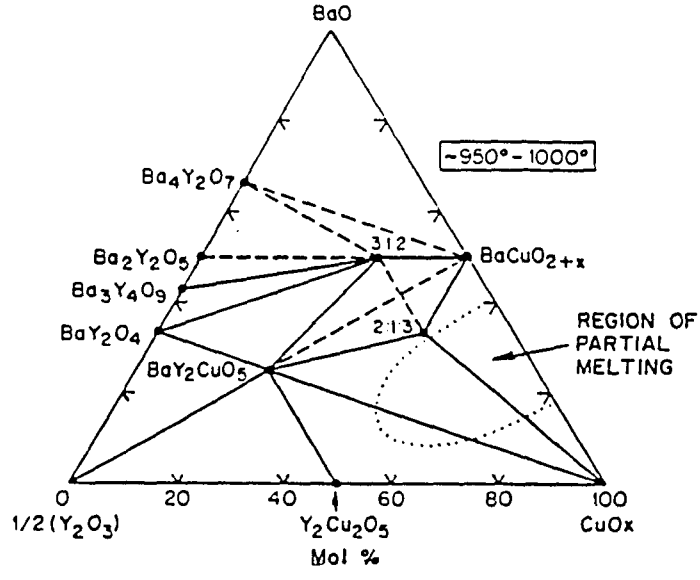

FIGURE 6: Ba-Y-Cu-O phase diagram for materials at 950° to 1000°C in air. Of interest to many researchers in preparing single crystals is the region of partial melting.

several days to several weeks. The crystals produced however were not large enough to make accurate resistance measurements on.[45,46] They are typically 0.5 X 0.5 X 0.2 cm. in size.

A second problem with all the superconducting ceramic systems is the transportation of electricity through the material. The current densities must be large in order to be beneficial for using. In bulk samples 10^7 or greater A/cm^3 were expected, however much lower than that has been achieved, typically 10^4 A/cm^3. In thin film samples, I_c densities of 10^6 A/cm^3 have now only recently been achieved.

A third problem with the processing of these ceramic superconductors is oxygen stoichiometry. For the $Y_1Ba_2Cu_3O_7$ system, the oxygen stoichiometry of the superconducting phase must be seven. As the oxygen stoichiometry decreases to six, the superconducting properties become weaker. From Figure 7, the superconducting structure can be seen for the $Y_1Ba_2Cu_3O_7$ phase.[47] Note the channels that are formed when the oxygen stoichiometry is seven. Proper oxygen stoichiometry is especially difficult in bulk samples, where the oxygen concentration gradient exist in the material. This makes a standard heat treatment schedule for these

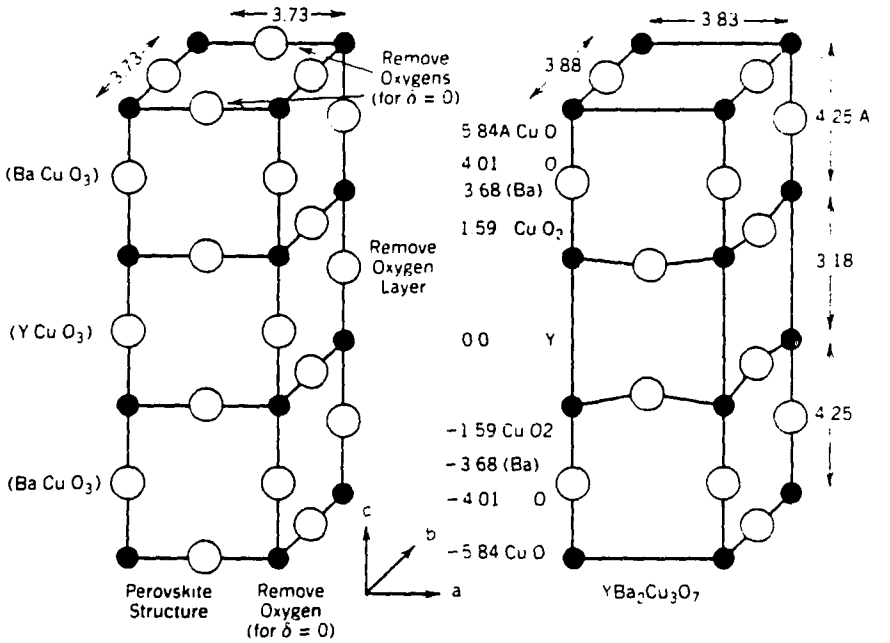

FIGURE 7: $YBa_2Cu_3O_x$ superconducting phase. (a) shows the non-superconducting phase, (b) shows the superconducting phase with the proper oxygen stoichiometry of x = 7.

superconductors very difficult. For bulk samples, heat treatment schedules call for holding the sample at temperature for periods of 10 hours to several days in order to minimize oxygen gradients. For thin films, however, the length of time the sample is held at temperature is only several minutes to an hour. Most heat treatment is done in an oxygen enriched atmosphere.

The emphasis on the processing of the ceramic superconductors has now been focused on producing pure single phases and on grain boundary refinement. As discussed above this is not a trivial undertaking.

CHAPTER III. OBJECTIVE

The objective of this study is to optimize the processing parameters involved with producing high T_c superconducting Y-Ba-Cu-O and Bi-Sr-Ca-Cu-O thin films produced by spray pyrolysis processing.

CHAPTER IV. EXPERIMENTAL PROCEDURE

Two materials systems were investigated based on the currently investigated superconductor phases being studied worldwide. Y-Ba-Cu-O and Bi-Sr-Ca-Cu-O based ceramic systems were the major focus of our experimental work. Solutions were prepared and sprayed onto a heated substrate (100-600°C) as is typical in SPP. The solution was sprayed for ten minutes and then turned off for one minute to allow for better pyrolysis. Total deposition time was 30-60 minutes. After spraying, the films were maintained at temperature for ten minutes to allow for continued pyrolysis. The carrier gas was left on at a lower flow rate and the solution flow was turned off. The films were then allowed to cool to room temperature. This took approximately one hour.

Details of equipment design, solution preparation, and the tailoring of precursor chemistry are first described followed by a summary of the analysis techniques used.

IV. A. Equipment Design

Due to the acidity of the spray solution and in order to minimize any metallic contamination, lucite and tygon tubing were used in the solution handling apparatus. The spray hood was designed so as to minimize air currents, which affects the deposition characteristics. The hood was a plexiglass cube with interior dimensions of 0.3 x 0.3 x 0.3 m. A door was installed in one side of the hood for easier access to the substrates and the spray nozzle. Initially a metal ring stand was used to support the spray nozzle inside this chamber. Due to possible metal contamination, a hole was cut in the center of the top of the chamber and the body of the nozzle was placed on the outside of the chamber.

The spray nozzle was a pressure fed lucite nozzle supplied by Spraying Systems, Inc. (Model No. 1/4J). A schematic of the spray nozzle is shown in Figure 8. The round spray pattern was chosen for best overall coverage. The fluid cap had an opening of 1.27 mm and the air cap had an opening of 1.70 mm. The round spray pattern created a spray diameter of 15 cm. The diameter was dependent upon the carrier gas flow and delivery pressure.

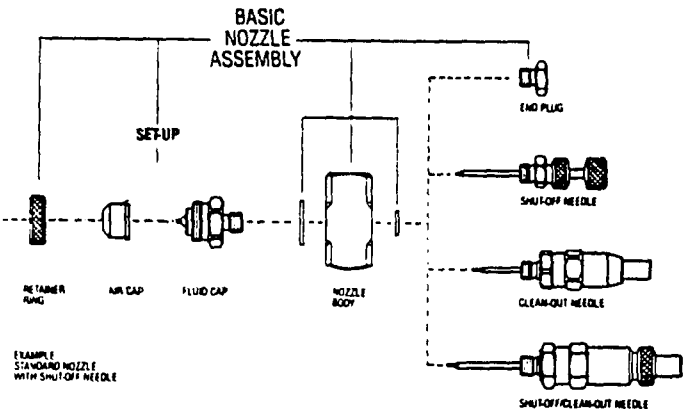

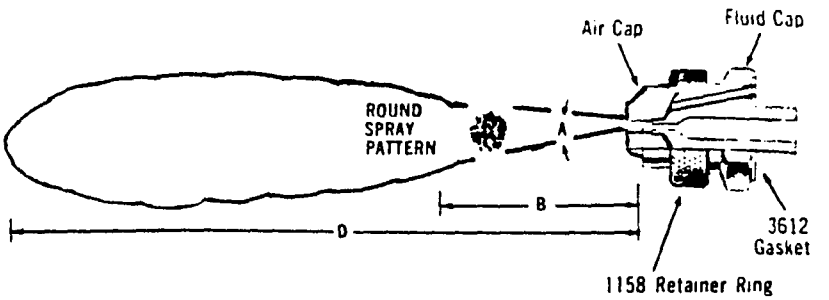

FIGURE 8: Breakdown of the spray nozzle used in the SPP of superconducting thin films.

The design and choice of an appropriate substrate heater is critical to the success of SPP. Initial experiments with a stainless steel block showed that heat transfer was inadequate and thus a chrome plated copper block was used in succeeding experiments. The copper block was heated by two Watlow cartridge heaters.* One cartridge heater had an integral J type thermocouple, which was used as the control thermocouple. Measurement of the surface temperature was accomplished by a thermocouple placed 0.3 cm below the surface of the copper block. This temperature was recorded as the surface temperature with fluctuations held to within ± 5°C. The block was wrapped in insulation except for the top surface and placed in a stainless steel box with a rectangular slot. The heater was then placed entirely inside the plexiglass spray hood.

IV. B. MATERIALS AND SOLUTION PREPARATION

As-received and polished substrates of Al_2O_3, MgO, and pyrex glass were used in this study. Typically four substrates per run were used to allow comparison of film quality as a function of location in the SPP chamber.

---

*Watlow Electric Mfg. Co., 12001 Lackland Rd., St. Louis, MI 63146

Spray solutions were prepared by dissolving stoichiometric quantities of the acetates, nitrates, oxides and/or pure metals in triple distilled, deionized water. Sources of chemicals are listed in Appendix III. The individual oxides and the pure metals were dissolved separately in nitric acid and then mixed together. The pH and Eh were checked to assure stability. From Figure 9, the stability region for the bismuth system is pH < 5 and Eh > 1.1 eV. Ammonium hydroxide was used to adjust the pH and hydrogen peroxide was used to adjust the Eh. Triple distilled deionized water was added to produce a one liter solution. An overall molarity of between 0.01-0.1 M was used.

IV. B. 1. SPECIAL CONSIDERATIONS

For the Y-Ba-Cu-O system, barium nitrate would not dissolve easily in water or nitric acid. The water was heated and the barium dissolved but, unless the solution was sprayed within twenty four hours, the barium would begin to precipitate out as a hydroxide.

In the case of the Bi-Sr-Ca-Cu-O system, bismuth was a problem. Bismuth nitrate would not dissolve in water, so

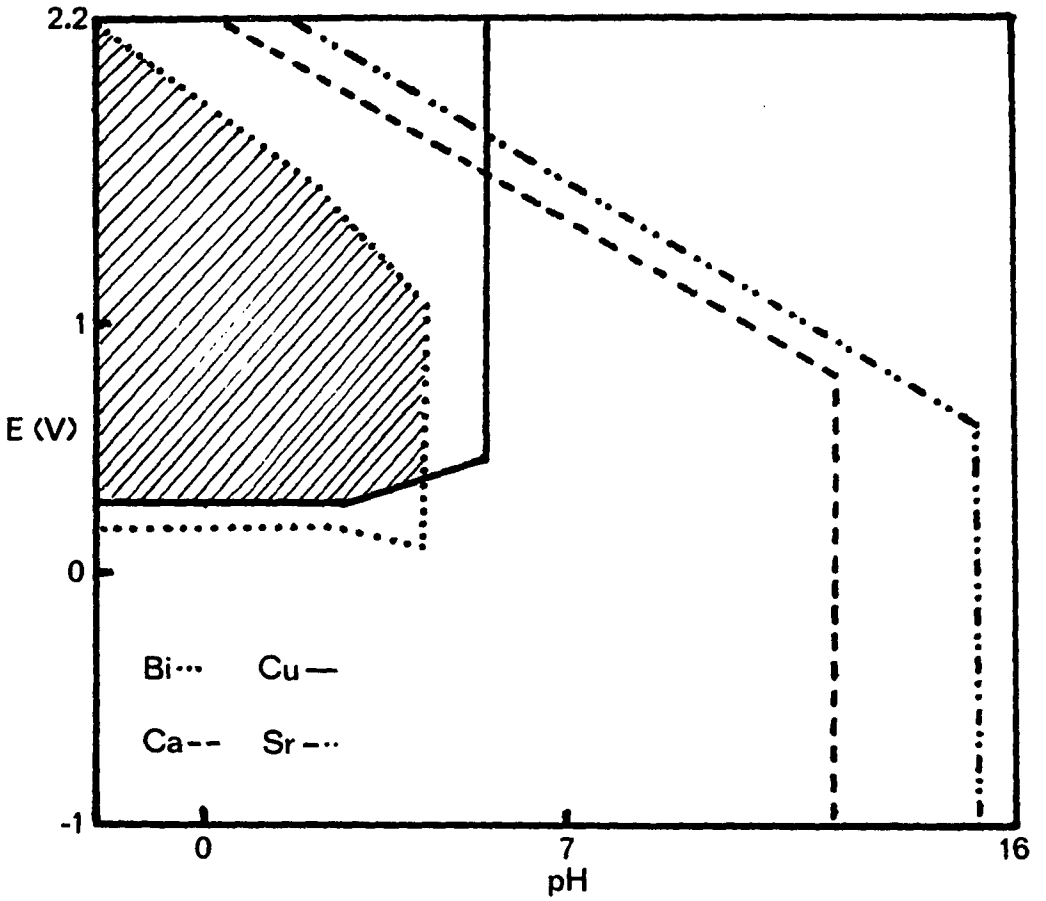

FIGURE 9: Compilation of Eh-pH diagrams for Bi, Ca, Cu, Sr, and water. The shaded area represents the stable region for all four species in water.

bismuth oxide dissolved in concentrated nitric acid was used.

The hygroscopic nature of the nitrates did create a problem with accurate weighing. When exposed to air for a short period of time these nitrates absorb water very quickly. Oxides were tried but the amount of nitric acid used to dissolve them was substantial and corrosion of the substrate heater becomes a concern. Therefore, a mixture of oxides, nitrates and pure metals was used.

IV. C. METHODS OF ANALYSIS

There were three methods used to analyze the films produced; X-Ray Diffraction (XRD), Scanning Electron Microscopy (SEM), and Rutherford Backscattering Spectrometry (RBS). As-deposited and heat treated films were characterized by these methods.

IV. C. 1. X-Ray Diffraction

X-ray diffraction was used to determine the crystallinity and the phases present in the films. A

General Electric XRD-5 x-ray diffractometer** was used to obtain an x-ray diffraction intensity versus 2θ for the films. Films were placed in the diffractometer sample holder and scanned at 2°/min using monochromatic Cukα radiation with a Ni filter. Source beam slit was 3° MR and the detector slit was MR. Several samples were too thin to provide accurate information. The JCPDS file system was used to index the peaks.

IV. C. 2. Optical and Scanning Electron Microscopy

The SEM was used to determine the surface morphology and microstructure of the films. An ISI*** Super IIIA SEM was used. Samples were grounded to the specimen holders using silver paste on the edges of the films. The optical microscope, an Unitron ZSM optical microscope was used to check for pinholes, lack of coverage and other macroscopic defects.

**General Electric Corp., X-ray Department, Milwaukee, WI (Note: No longer in business)

***International Scientific Systems, Inc. 3255-6C Scott Blvd, Santa Clara, Ca 95050

IV. C. 3. Rutherford Backscattering Spectrometry

RBS was used to determine the concentrations of the various species in the film. A 5.5 MV Van de Graaff particle accelerator operated by the Physics department at the University of Arizona. Prof.'s J. A. Leavitt and L. C. McIntyre, Jr. and students performed the tests. Figure 10 is a schematic diagram of the setup used

A $^4He^+$ ion beam was accelerated at the film. A high energy beam ion was used (3776 KeV) in order to penetrate the thick films. Most of these ions pass into the film and come to rest several microns into the substrate. Several of these He ions are backscattered from both the film and the substrate. These backscattered ions are collected at an angle 170° from the incident ion direction by a detector. The signal is then processed through a preamp, amp and then a multi-channel analyzer. A typical resultant spectra is shown in Figure 11. In order to produce a good signal from the film, a low atomic number substrate material is normally required. In this case the alumina substrates made the measurement of oxygen stoichiometry impossible.

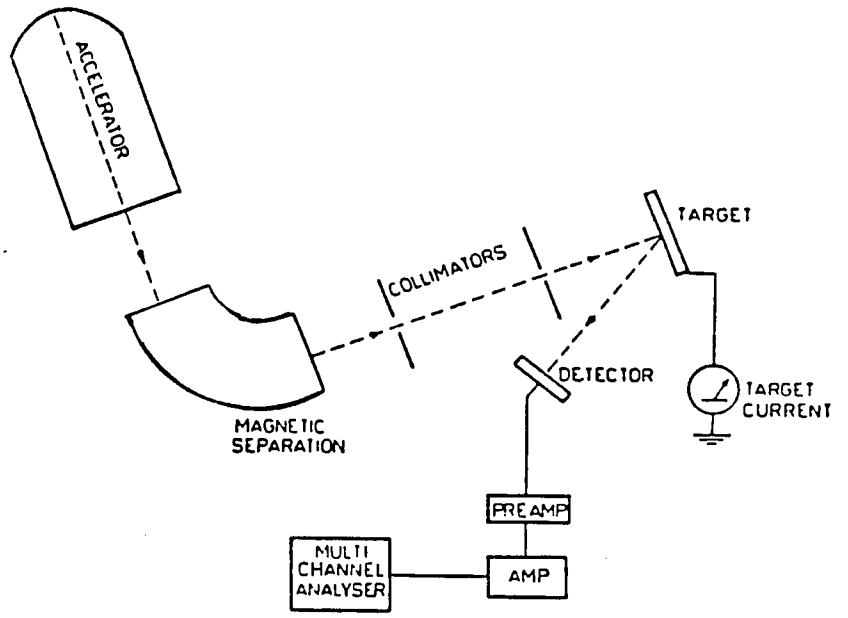

FIGURE 10: Schematic of RBS set-up used to determine composition of thin films.

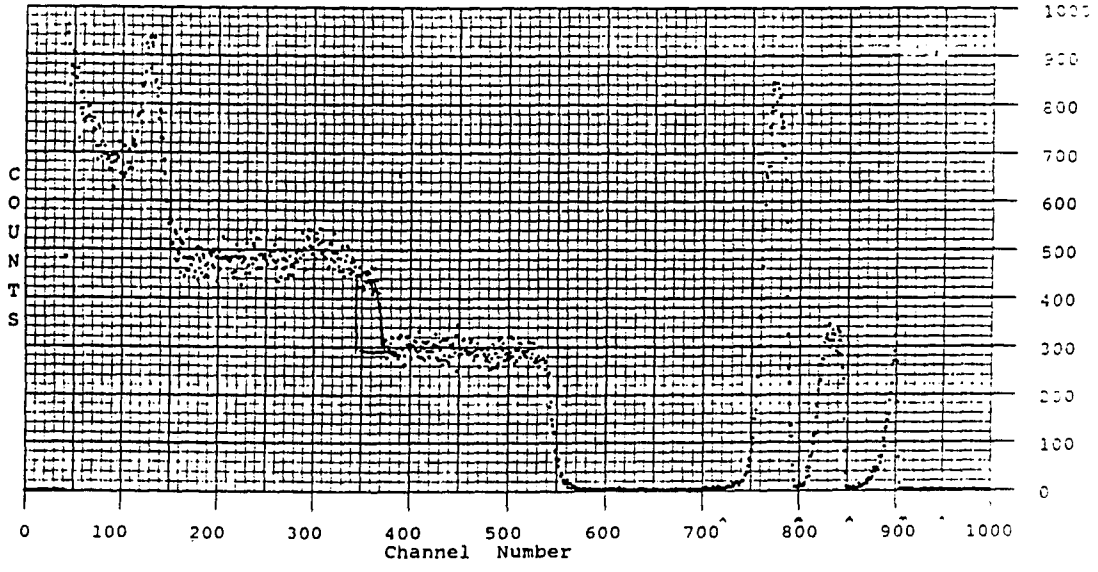

FIGURE 11: Typical 3.8 MeV $^4He^+$ RBS spectra obtained for Y-Ba-Cu-O thin films.

From the backscattering integrated spectrum, areal densities (in atoms/cm^2) were obtained for each element in the film. The physical thickness was then estimated by assuming individual layers of the pure elements and a bulk density for each density. The thickness of each of these layers was calculated as follows;

$$t = (N_t)_i * (A)/[(\rho_i)*(N_a)]$$

where t is the thickness in cm.,
N_t is the atoms/cm^2 for each element
as determined by RBS,
A is the atomic weight,
ρ_i is the bulk density in g/cm^3, and,
N_a is Avogadro's number.

The individual thicknesses are then summed to obtain the overall thickness. Accurate measurements of films with thicknesses >200 nm was not possible due to overlapping peaks with varying shapes caused by non-uniform concentrations. Values obtained for stoichiometry were typically $\pm$10%.

Chapter V: RESULTS AND DISCUSSION

V. A. Y-Ba-Cu-O System

Preliminary experiments were performed on superconducting compositions in the Y-Ba-Cu-O system, commonly referred to as the 1-2-3 system. Table IV shows the optimized SPP parameters for deposition of these films, as developed in the present study.

Films for in the Y-Ba-Cu-O system were deposited at a temperature of <400°C onto glass, MgO, and Al_2O_3 substrates. As deposited films varied in color from brown to black and were free from obvious macroscopic defects such as pinholes. SEM analysis revealed an uneven surface morphology most likely due to incomplete pyrolysis although complete coverage of the substrate was obtained as seen in Figure 12(a). Upon heat treatment, SEM revealed the films were cracked extensively (Figure 12(b)), due to the mismatch in the coefficients of thermal expansion of the film and the substrate (13.6 X 10^{-6}/°C for $YBa_2Cu_3O_7$ and 0.5 X 10^{-6}/°C for silica glass).[6] MgO substrates, with a coefficient of thermal expansion of 12.8 X 10^{-6}/°C, were subsequently used, to solve the cracking problem.

TABLE IV: Experimentally Optimized Processing Parameters for Processing of Y-Ba-Cu-O Thin Films by Spray Pyrolysis

Solution Flow Rate	1 ml/min.
Carrier Gas Flow Rate	44 l/min.
Substrate Temperature	336°C
Substrate to Nozzle Distance	28 cm.
Substrate	MgO
Solution Molar Concentration	0.01 M
Starting Materials	Nitrates

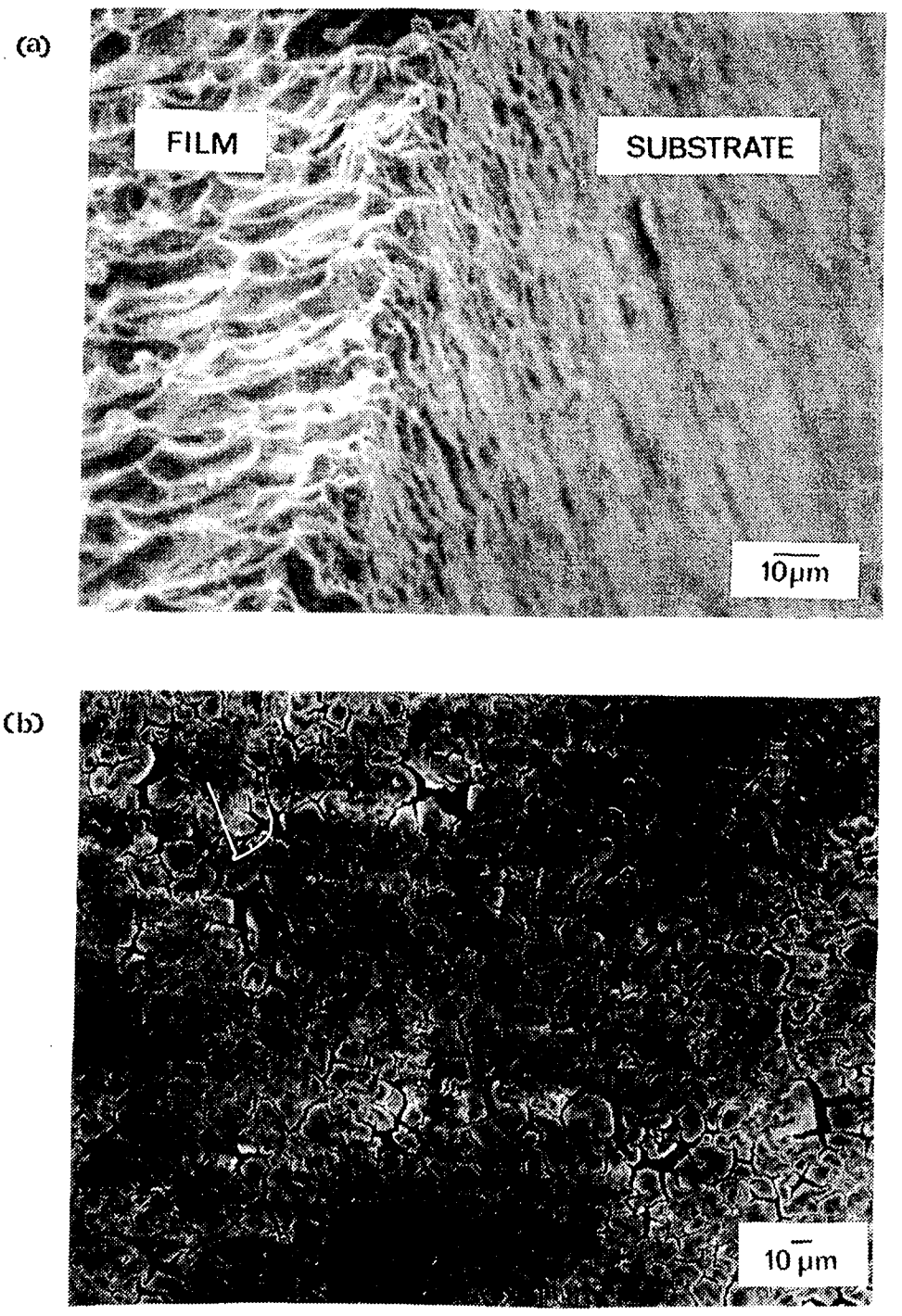

Figure 12 (a and b): SEM micrographs showing (a) as deposited film tilted at 70 degrees, and, (b) heat treated sample with extensive cracking.

V. A. 1. RBS and XRD RESULTS

RBS results showed the films produced on silica substrates to be deficient in both barium and yttrium. Table V and Figure 13 shows the results of the as deposited films, showing the decrease in both barium and yttrium with increasing substrate temperature. The barium peak in the RBS spectra (Figures 14-18) shows an exponential shape rather than a rectangular shape. The difference in the shapes of these spectra is due to thickness differences. Figures 15, 17, and 18 are much thinner films than Figures 14 and 16, as evidenced by the presence of individual sharper peaks. Interpretation of this shape suggests that the barium is either diffusing into the substrate or migrating to the surface by an unknown mechanism. The apparent enrichment of the barium at the surface of the films, suggested by the RBS results, can be explained by assuming that the freshly deposited barium on the surface does not have adequate time to diffuse through the film into the substrate. However, the underlying barium layers deposited in the early stages of SPP can diffuse during this same time interval.

TABLE V: RBS Data of Spray Pyrolysis Films on Silica substrates from a 1:2:3 starting solution stoichiometry

Temperature (°C)	Stoichiometry Y	Ba	Cu
203	1.7 ± 0.6	1.2 ± 0.4	3
235	1.3 ± 0.4	1.4 ± 0.2	3
292	1.17 ± 0.15	1.05 ± 0.12	3
301	0.89 ± 0.1	0.07 ± 0.02	3
376	0.62 ± 0.1	0.03 ± 0.01	3
600	nothing detectable		

Copper stoichiometry set equal to 3 for ease of comparison. Measurements were taken at the top surface of the film, the top 200-500 Angstroms.

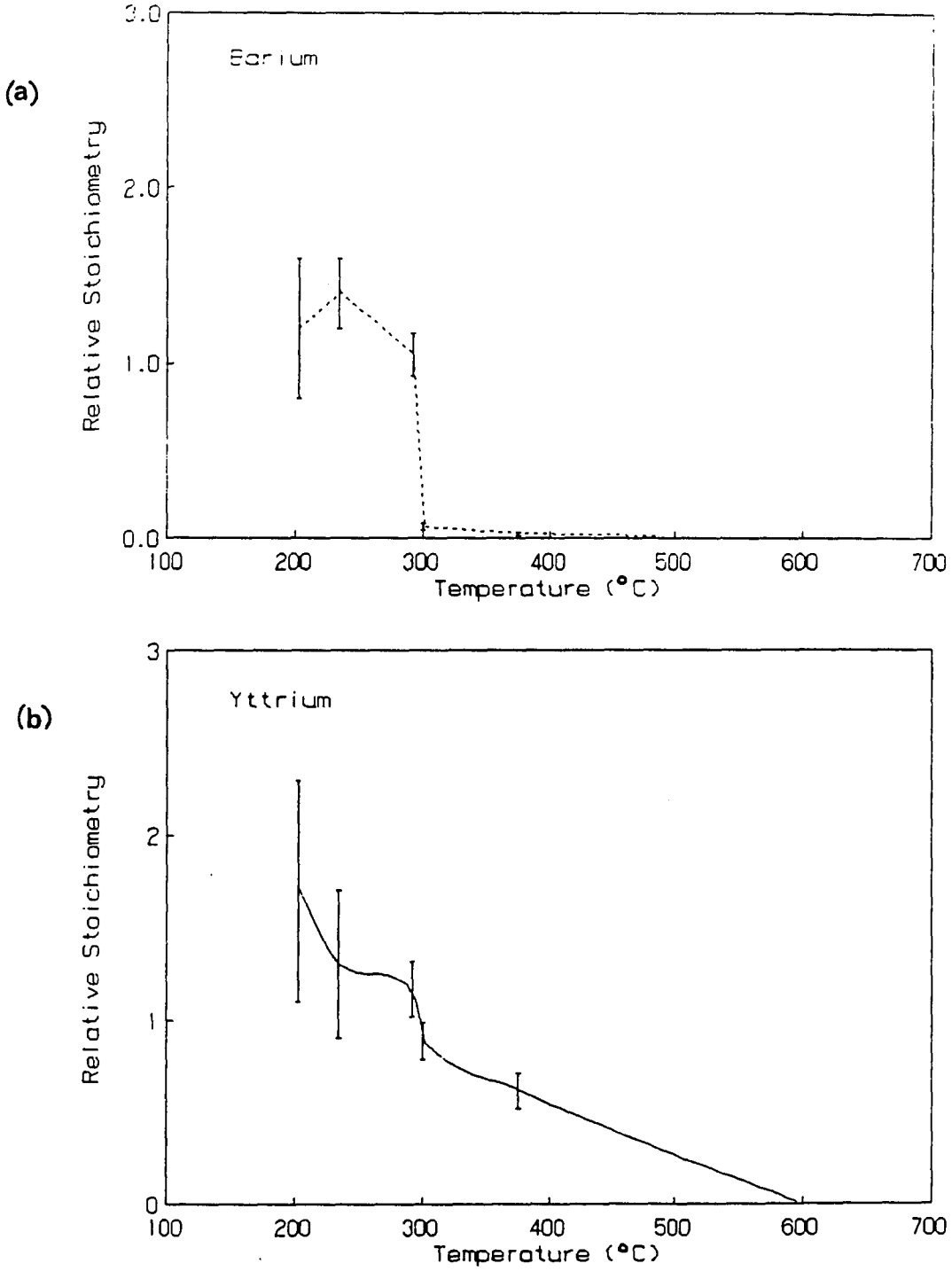

FIGURE 13 (a and b): Plots of relative stoichiometry vs temperature for barium and yttrium from RBS results.

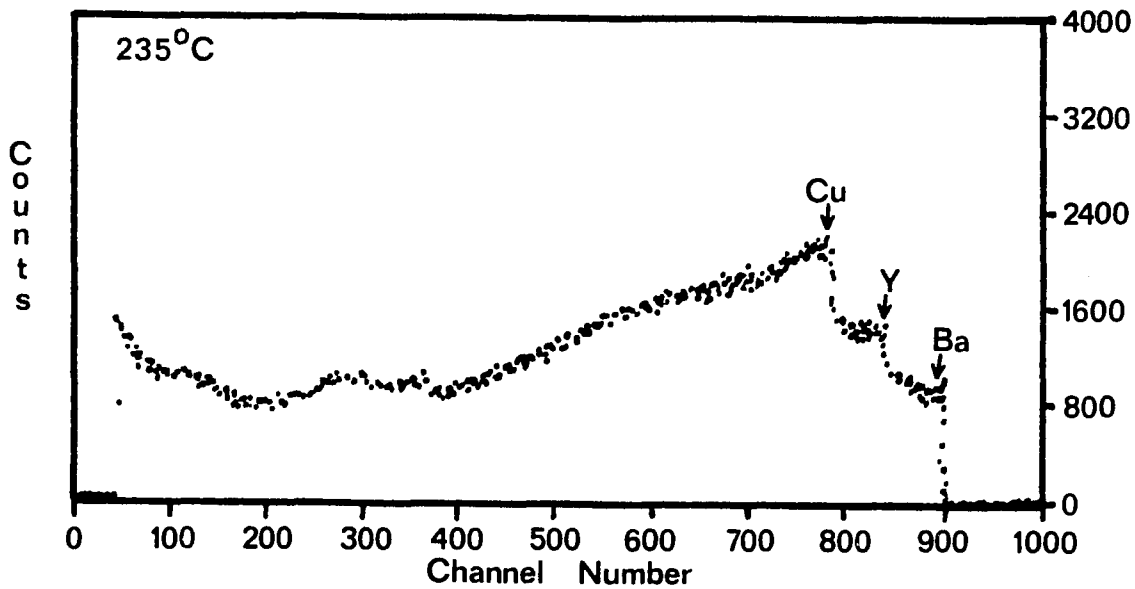

FIGURE 14: 1.9 MeV $^4He^+$ RBS Spectra of as deposited Y-Ba-Cu-O thin film.

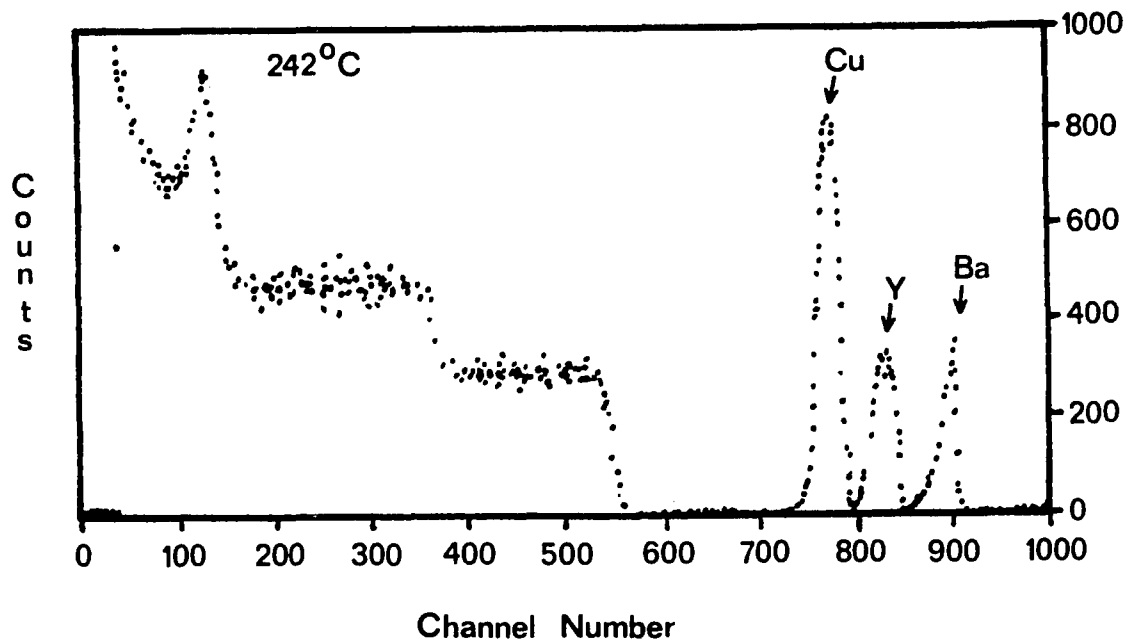

FIGURE 15: 3.8 MeV $^4He^+$ RBS Spectra of as-deposited Y-Ba-Cu-O thin film.

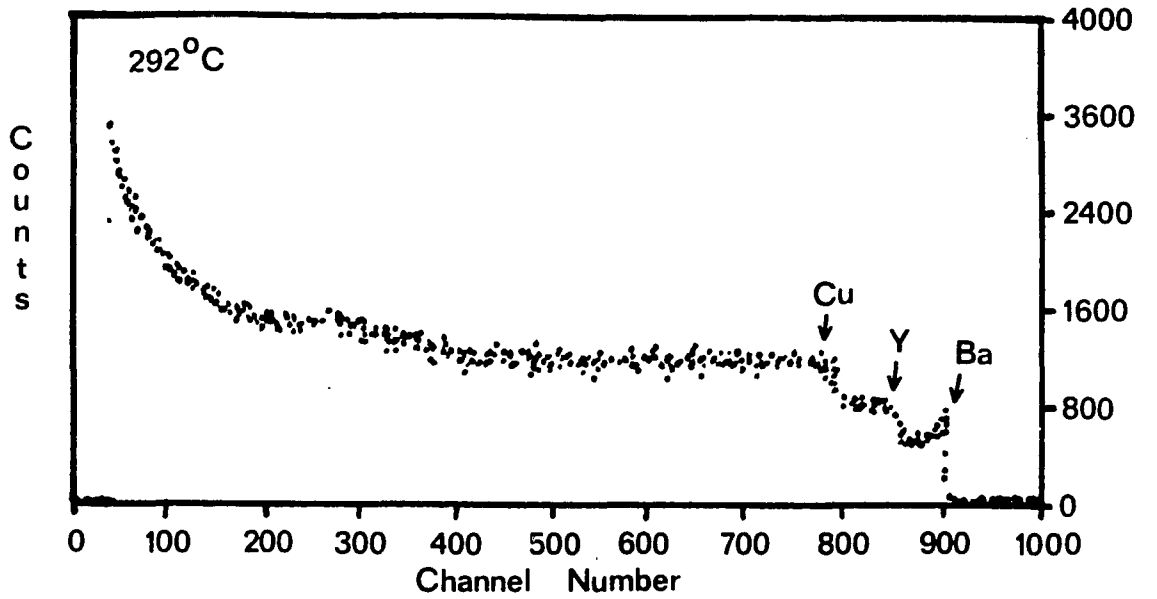

FIGURE 16: 1.9 MeV $^4He^+$ RBS Spectra of as deposited Y-Ba-Cu-O thin film.

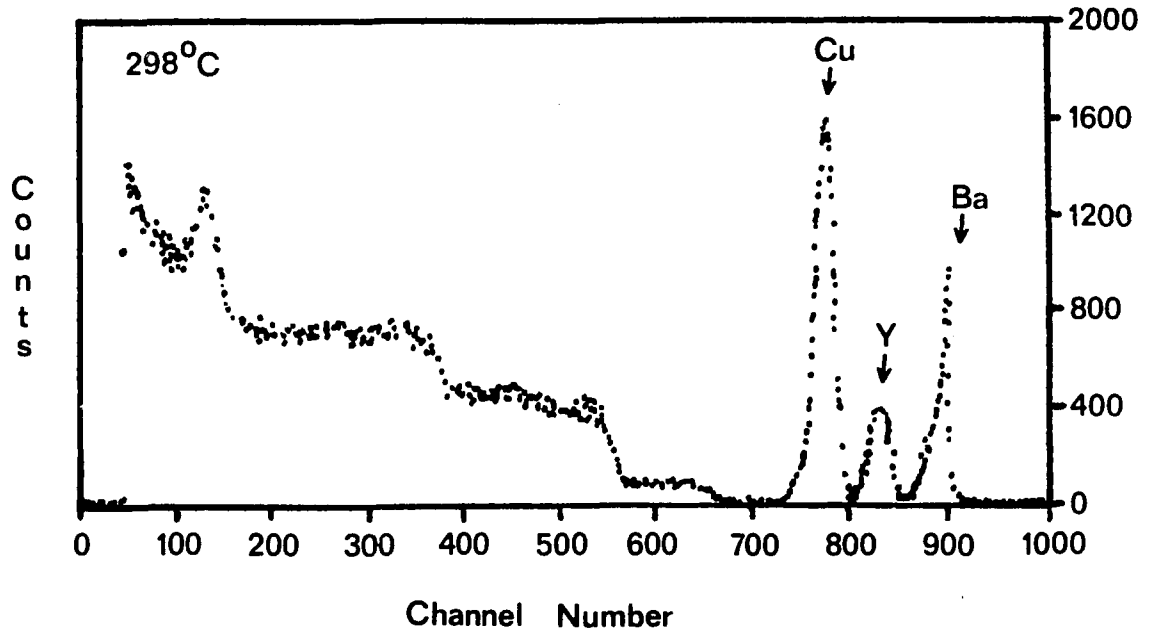

FIGURE 17: 3.8 MeV $^4He^+$ RBS Spectra of as-deposited Y-Ba-Cu-O thin film.

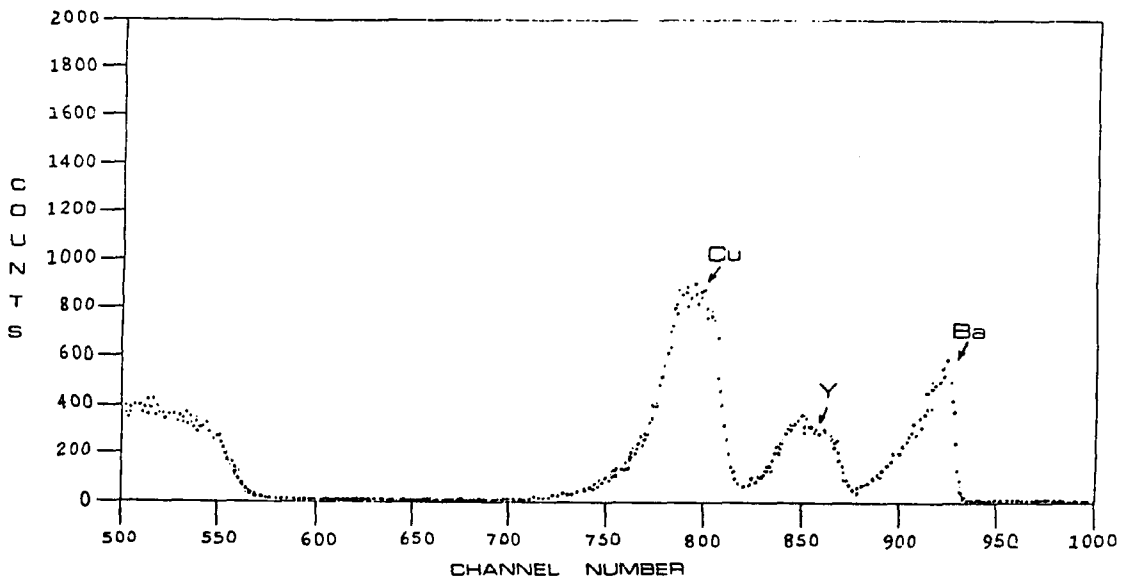

FIGURE 18: 3.8 MeV $^4He^+$ RBS Spectra of as-deposited Y-Ba-Cu-O thin film. Note the exponential shape to the barium peak. This indicates either diffusion or islanding.

Barium diffusion in films and bulk oxide ceramics has been reported in the literature, providing some evidence for barium diffusion into the silica substrates in the current series of SPP experiments.[19,48,49] Barium does form a silicate quite readily and the possibility that a barium silicate was formed by some film/substrate interface reactions may explain the observed barium deficiencies in the films. Such silicate formation may be in an interfacial layer too thin for detection by XRD and may require further high resolution electron microscopy data.

Previous studies have shown that when iron is deposited onto a Y-Ba-Cu-O superconductor, the barium diffuses into the iron film and the interface composition is non-uniform mixture of barium and iron.[48] It is thus possible that an amorphous or disordered mixture of barium and silica, as opposed to a crystalline barium silicate, forms at the interface in the present SPP experiments.

Other materials which had been found to have this interfacial diffusion problem include iron, strontium titanate, zirconia, and alumina. In order to alleviate this diffusion problem, the use of barrier layers has been suggested. For depositing the 1-2-3 system on cubic

zirconia, silver has been used as a buffer layer.[19] While other barrier layers and substrates include, niobium on magnesium oxide, silver on zirconia, and $YBa_2Cu_3O_7$ on itself.[48] No attempt to investigate barrier layers was made in the present work.

Results obtained by SPP on MgO substrates provided encouraging evidence for the formation of the desirable 1-2-3 phase. Samples deposited on MgO substrates were heat treated at 920°C for 1-2 hours. The heat treated samples, analyzed by XRD, showed ten peaks which closely matched the desired 1:2:3 superconductor (Figure 19). Table VI is a comparison of the d spacings of the phase obtained with the known superconducting phase is in the Y-Ba-Cu-O system. From Table VI, the d-spacings for another phase was also present but has yet to be identified. Secondary phases are not uncommon when processing these complex materials and the attainment of stoichiometry and homogeneity remain crucial processing challenges in SPP.

Following the preliminary work on the Y-Ba-Cu-O series research was continued on the new Bi-Sr-Ca-Cu-O system. Not only are the superconducting transition temperatures higher in this system, but greater critical current

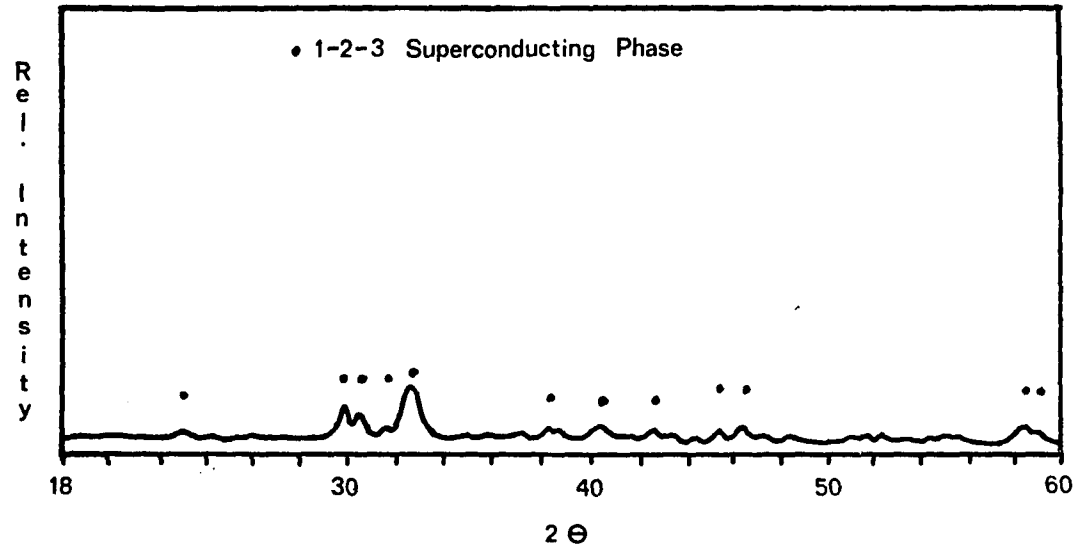

FIGURE 19: XRD traces of a SPP produced Y-Ba-Cu-O thin film which closely matched a 1:2:3 superconductor.

TABLE VI: d-spacing Comparisons for a Heat Treated Y-Ba-Cu-O Film. (Note: Substrate peaks have been excluded)

2θ	$d_{(experimental)}$ (Å)	$d_{(calculated)}$ (Å)	delta d
23.0	3.8635	3.8900(003)	0.0265
30.0	2.9760	2.9900(---)	0.0140
30.7	2.9693		
31.8	2.8115	2.8270(---)	0.0155
32.9	2.7200	2.7290(103)	0.0090
38.7	2.3247	2.3360(005)	0.0113
40.9	2.2046	2.2320(113)	0.0740
43.0	2.1016		
45.8	1.9794	1.9480(006)	-0.0314
46.8	1.9383	1.9480(006)	0.0097
48.8	1.8645		
58.4	1.5788	1.5700(213)	-0.0088
59.2	1.5594	1.5860(116)	0.0206

(Source: Longsworth, R.C., et. al., "Observations of the Deterioration of $YBa_2Cu_3O_7$ Using a New Superconductor Characterization Cryostat," High Temperature Superconducting Materials Preparations, Properties, and Processing, W.H. Hatfield amd J.H. Miller, Jr., eds., Marcel Dekker, Inc. (1988))

densities have been reported.

V. B. Bi-Sr-Ca-Cu-O System

The knowledge and experience gained in the SPP of the Y-Ba-Cu-O system provided a useful database for the spray pyrolysis processing of superconducting oxides in general. From this experience, an SPP investigation of the Bi-Sr-Ca-Cu-O superconducting system was performed, with a major emphasis on solution preparation prior to spraying.

V. B. 1. Optimization of Processing Parameters

In the optimization of the processing parameters for the Bi-Ca-Cu-Sr-O system, solution chemistry and preparation is crucial. As the number of components in solution increase, the complexity of the solution preparation increases. Therefore, a more scientific approach to solution preparation prior to spraying was given in this part of the study was needed. The differences in solution preparation from the Y-Ba-Cu-O system are discussed below.

V. B. 1. a. SOLUTION PREPARATION

Eh-pH diagrams were studied to determine a stability region for the four components. Figure 20 is a compilation of the bismuth, calcium, copper, and strontium ions in water, the individual diagrams are shown in Appendix IV.[50] Although this does not include the nitrate ions, the diagram does provide a processing window for solution preparation.

Several methods were used for solution preparation. Initially, all four nitrate species were dissolved in distilled water, however several variations were necessary to produce a stable solution without the formation of precipitates. These variations include the following: (a) nitric acid was necessary to completely dissolve the bismuth nitrate, (b) copper acetate was substituted for the copper nitrate due to the inaccuracies of weighing the hygroscopic copper nitrate, and (c) the pH of the solutions was quite low, less than pH = 1, so ammonium hydroxide was used in order to raise the pH to above 2.5. The Eh of the solution was normally within the stability region, so that further adjustments to it were not necessary. Films were successfully produced from both the all nitrate and the acetate/nitrate solutions.

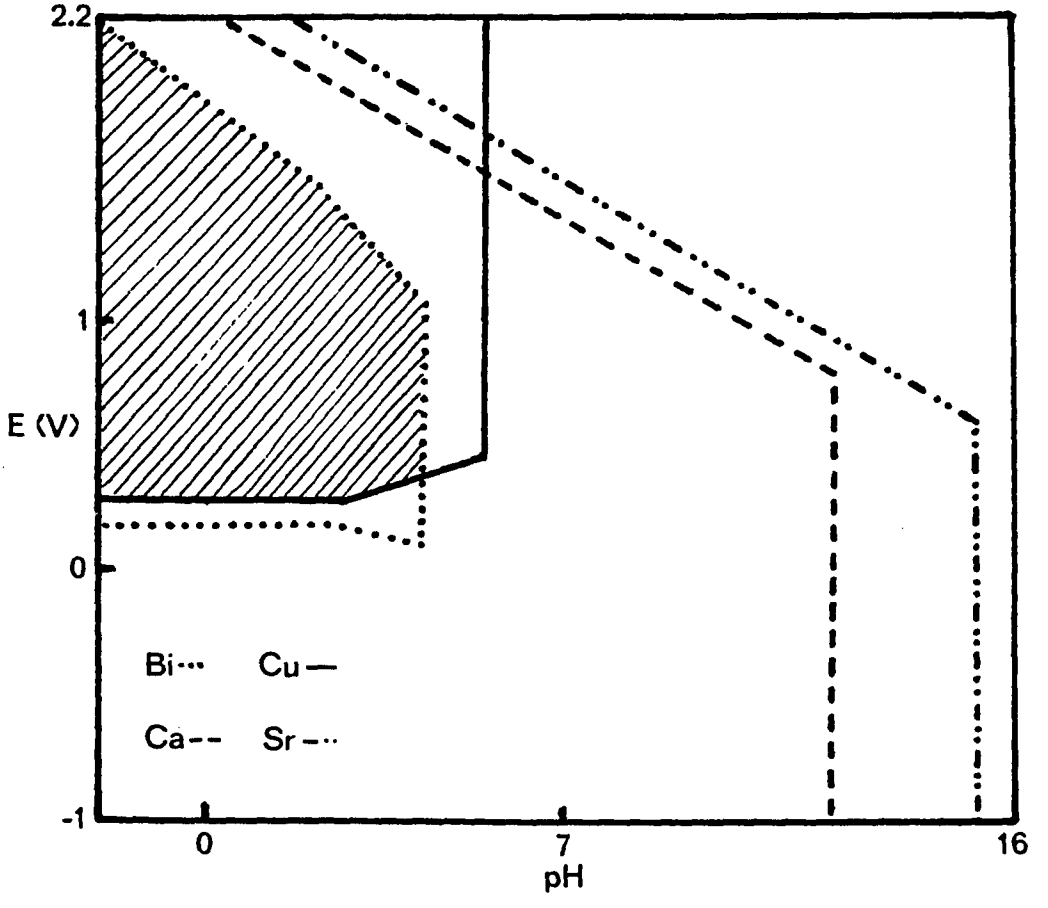

Figure 20: Eh-pH diagram of Bi, Sr, Ca, and Cu in water. The shaded area is the processing window, where all four species are stable in solution.

Another method to prevent undesirable precipitation in the SPP solution when using the nitrate solutions was based on a review of hydrometallurgical techniques, for recovering metals via wet chemistry. A complexing or chelating agent such as ethylenediaminetetraacetic acid (EDTA), is used for recovering metal species from solutions, as in flotation, where the unwanted metal species are complexed and stay in solution while the desired metal to be recovered is floated to the surface and skimmed off. The purpose of this complexing agent is to attach itself to the free cation and not allow it to form a precipitate, in the form of an insoluble hydroxide. Figure 21, shows the way in which the chelating agent engulfs the cation, protecting the cation from its surroundings and not allowing it to precipitate.[51] EDTA is very pH sensitive and must be constantly monitored. EDTA was tried in the latter stages of this study, but the solutions gelled after standing for several hours due to an imbalance between the pH, Eh, and EDTA concentration. Further investigation into this balance is needed if EDTA is to be considered as an additive.

Other solutions were produced from dissolving the oxides in nitric acid. But, as was discovered with the Y-Ba-Cu-O system, the acidity of these solutions was too low, causing

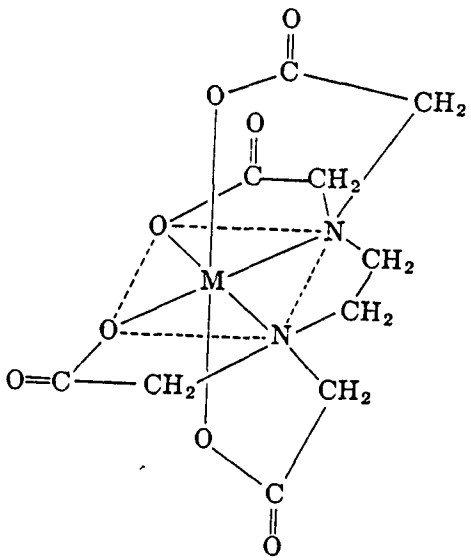

Figure 21: EDTA chelating agent. The M represents the metal ion surrounded by the EDTA complex.

accelerated corrosion of the substrate heater. Ammonium hydroxide was used to neutralize the acid. Films produced from these solutions were not of the same quality as the films produced from the nitrate solutions. This was due to the ammonium ion present in solution. Ammonium chloride and the metal chlorides were obtained in the films and upon heat treatment produced pores and pinholes in the films.

V. B. 1. b. Other Solution Considerations

In the Y-Ba-Cu-O system, there was a deficiency in the barium and sometimes in the yttrium concentrations of the films. The barium deficiency was likely due to the diffusion into the substrate. The diffusion of yttrium cannot be used to explain its deficiency. A possible explanation for the deficiency in the yttrium is the volatility of yttrium while it is being sprayed. It is plausible that the yttrium is evaporating either, prior to or during contact with the substrate. In either case, the higher the concentration of a particular species in the solution, the greater the chances of it being deposited onto the substrate. In conjunction with an overall higher concentration, a longer spray time can also increase the probability of deposition. Therefore, for this system a

more concentrated solution and longer spray times were used, increasing the probability for the desired materials to be deposited in the desired stoichiometry.

V. B. 2. RBS and XRD Results

Table VII is a compilation of the optimizied processing parameters for the Bi-Sr-Ca-Cu-O system. Since longer spray times and increased spray concentrations were used in this section of the study, accurate RBS results could not be obtained on a majority of these films, as the thicknesses was > 2 microns. Several films produced however were thin enough to be analyzed by RBS and the resultant spectra are shown in Figures 22 & 23 and Table VIII shows the RBS results of films sprayed onto Al_2O_3 for 0.5 hours using copper acetate instead of copper nitrate. These results show an exponential shape to the bismuth peak, not unlike the barium peak in the Y-Ba-Cu-O system. This, however, did not hinder the study of this system since higher solution concentrations and a larger solution flow rate was used. In addition to the bismuth peak, there is no calcium detected in the films sprayed at temperatures between 482°C and 600°C. An explanation for the lack of calcium can possibly be explained by the same argument used in the

TABLE VII: Experimentally Determined Optimized Parameters for Processing of Bi-Ca-Cu-Sr-O Thin Films by Spray Pyrolysis.

Solution Flow Rate	4 ml/min.
Carrier Gas Flow Rate	44 l/min.
Substrate Temperature	286°C
Substrate to Nozzle Distance	28 cm.
Substrate	Al_2O_3
Solution Molar Concentration	0.1 M
Starting Materials	Nitrates/Acetates

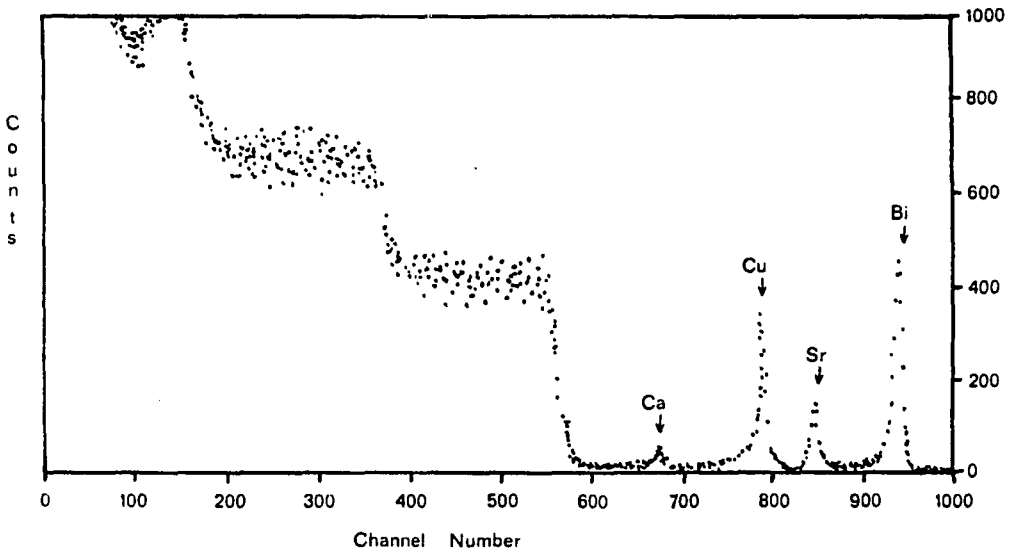

FIGURE 22: 3.8 MeV $^4He^+$ RBS spectra of a Bi-Sr-Ca-Cu-O thin film produced via SPP. The exponential peak of bismuth indicates possible diffusion into the substrate.

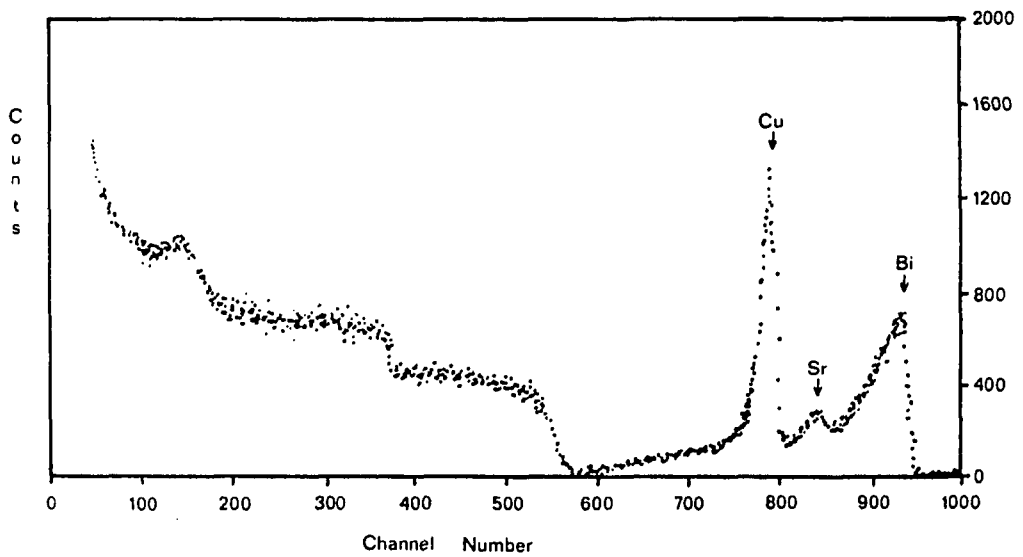

FIGURE 23: 3.8 MeV $^4He^+$ RBS spectra of a Bi-Sr-Ca-Cu-O thin film produced via SPP. The exponential peak of bismuth indicates possible diffusion into the substrate. Also note there is no calcium present.

TABLE VIII: RBS results of films sprayed from an all nitrate solution except for copper, which was present as an acetate. Results were standardized for bismuth = 1. Note the absence of calcium at 500°C and 550°C.

Temperature (°C)	Bi	Sr	Ca	Ca
186	1.00	2.00 ± 1.00	1.80 ± 0.50	3.50 ± 0.60
250	1.00	1.22 ± 0.09	14.02 ± 0.83	0.40 ± 0.17
290	1.00	1.09 ± 0.06	11.02 ± 0.25	0.79 ± 0.10
300	1.00	1.17 ± 0.14	6.30 ± 0.47	0.64 ± 0.22
500	1.00	0.82 ± 0.51	0.00	7.59 ± 1.74
550	1.00	4.38 ± 1.89	0.00	47.08 ± 10.41
600	1.00	1.23 ± 0.33	7.31 ± 1.13	0.63 ± 0.27

solution preparation section of this chapter. The calcium evaporates prior to or just after it contacts the substrate. It would follow that calcium is very volatile at the higher temperatures, and does not deposit on the substrate at the elevated temperatures. However at a substrate temperature of 600°C, the calcium peak reoccurs. The reoccurrence of the calcium peak has not yet been explained.

Films sprayed from the nitrate solutions were too thick to obtain accurate RBS results from, therefore XRD was relied on to provide information about these films.

Figures 24 & 25 are XRD traces of as-sprayed SPP films at temperatures from 130-482°C. These films are composed of multiple phases. At the lower temperatures (<236°C) the individual oxides, hydroxides and unpyrolyzed nitrates are present, also copper rich phases are prevalent. This can further be seen from Figure 26 which shows the color of the films to be changing from aqua to blue/black to a tan/black with increasing substrate temperature. The aqua color of the films is proof that copper rich phases are present. This strongly agrees with the XRD results that at lower substrate temperatures there is an abundance or predominance of copper or copper rich phases present. At the higher

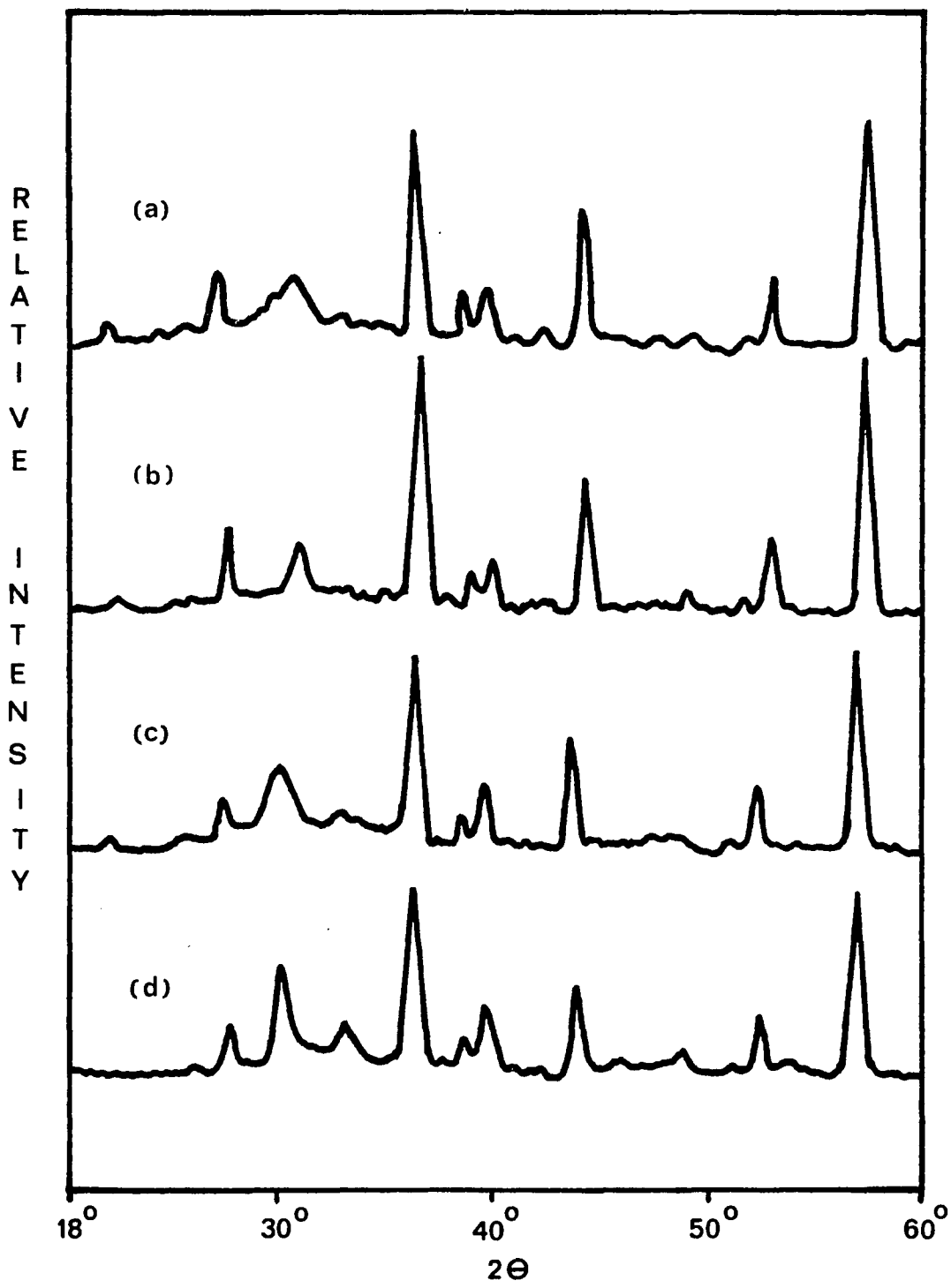

FIGURE 24: XRD traces of as-deposited SPP thin films deposited at (a) 130°C, (b) 186°C, (c) 236°C, (d) 286°C.

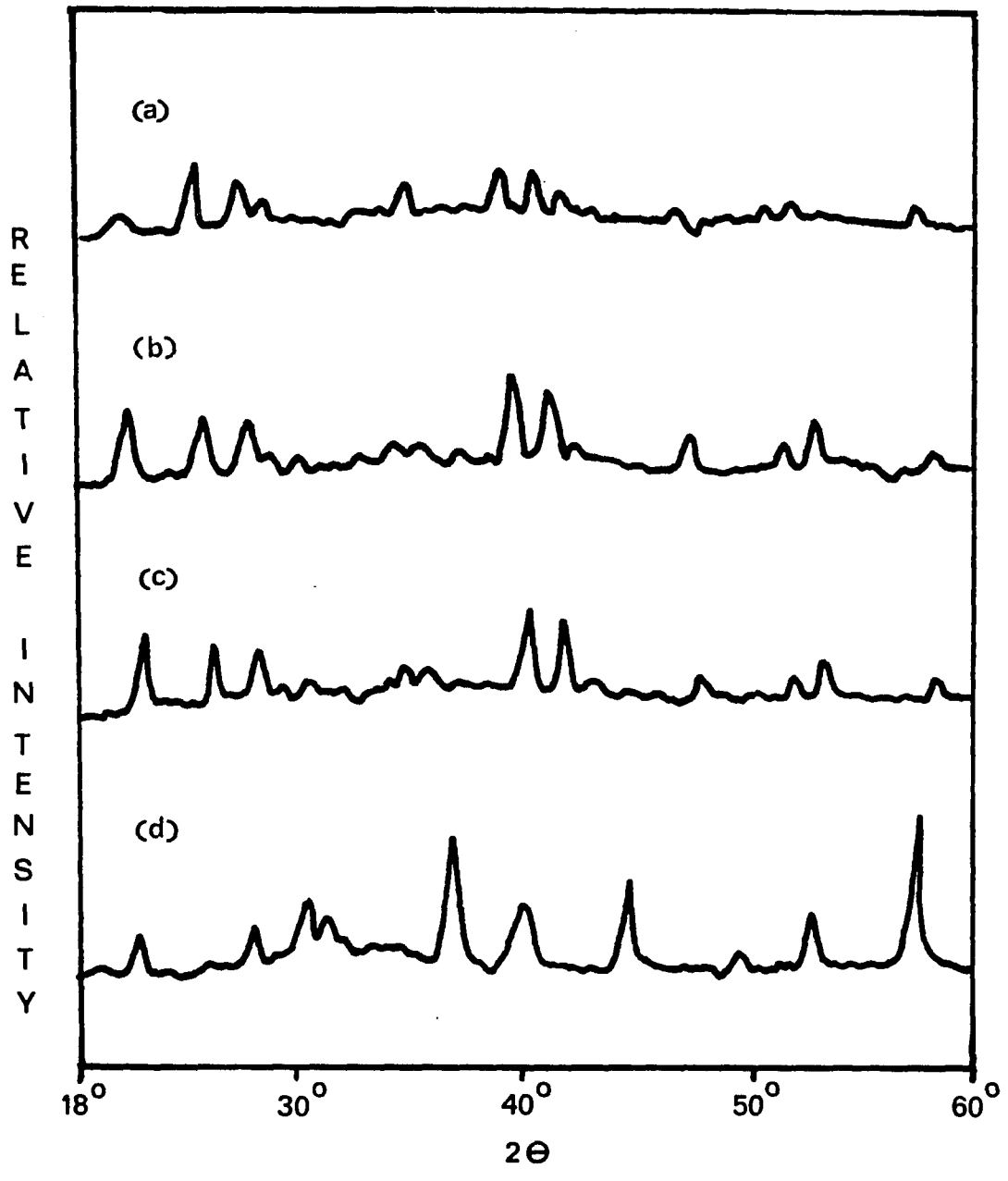

FIGURE 25: XRD traces of as-deposited SPP thin films deposited at (a) 336°C, (b) 386°C, (c) 425°C, (d) 482°C.

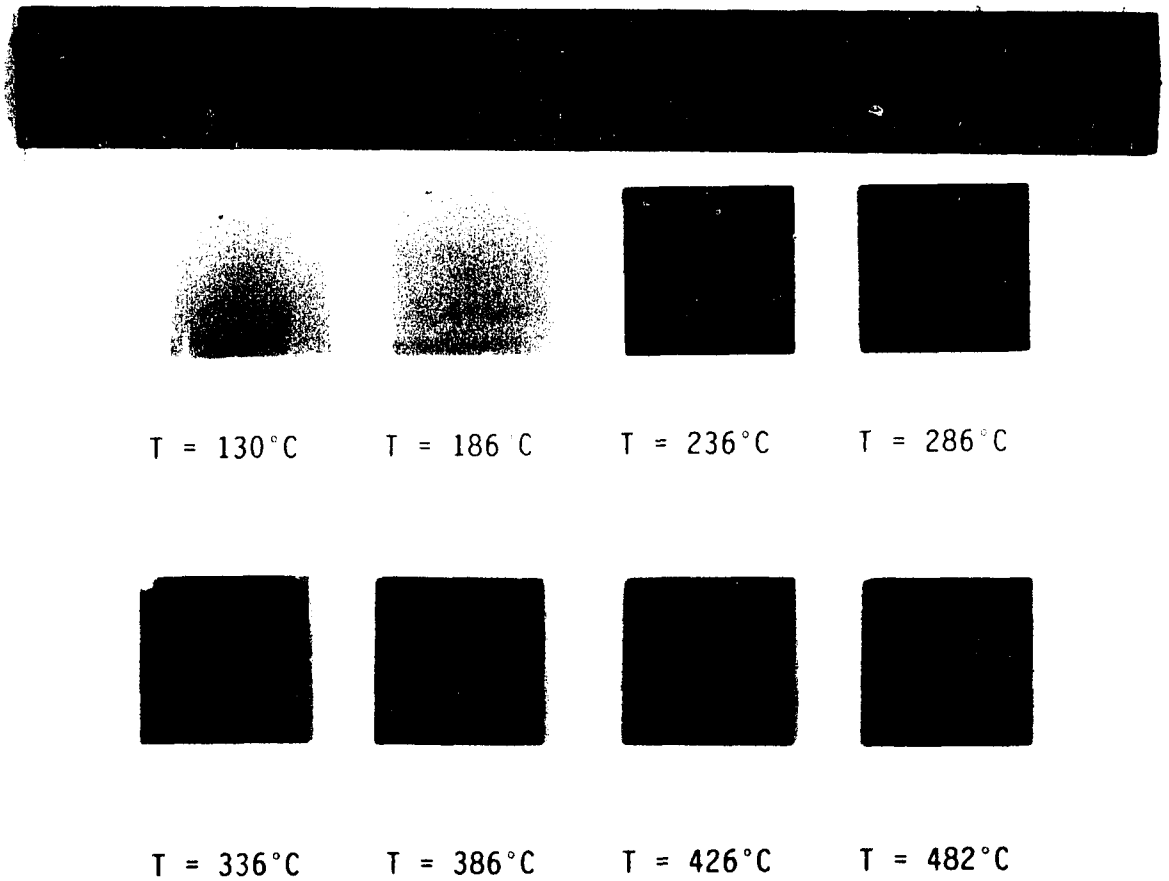

FIGURE 26: Photograph of films produced at various temperatures showing the color variations with temperature. Note the aqua to blue color of films produced at lower temperatures (<236°C).

temperatures, the oxides formed are of a multi-cation oxide variety and are not comprised of a dominant phase material (ie. copper rich phases). The multi-cation oxides are able to form due to the temperature being high enough for the cation to have greater mobility. The desired superconducting phases were not seen in the as-sprayed films. This was expected, since most processes used require a high temperature post-deposition anneal, to obtain the proper oxygen stoichiometry. Interestingly, in all films produced a $CaO_{0.33}SrO_{0.67}(NO_3)_2$ phase was present, as shown by XRD. This indicates complete pyrolysis is not occurring at temperatures less than 482°C. However, when higher temperatures were used, the loss or volatilization of calcium is observed. Therefore processing of SPP films in the Bi-Sr-Ca-Cu-O system must be done at temperatures less than 482°C followed by a careful heat treatment. It can also be seen that there are peaks which have not yet been identified. This is not surprising, since the Bi-Sr-Ca-Cu-O system has not been fully characterized for secondary defect structures, which may be present.

V. B. 3. Heat Treated Samples

A heat treatment schedule was developed by heat treating as-sprayed films at 500°, 600°, 800°, and, 825°C for 1.5 hours in flowing oxygen and examining them with XRD for the desired superconducting phases (Figures 27 & 28). Examining these figures, shows the superconducting phase beginning to appear at 500°C. At 600°C, other phases appear to develop and mask over the superconducting phase. At 800°C, the superconducting phase reappears as a dominant phase.

As mentioned previously, there are several phases in the Bi-Sr-Ca-Cu-O system which superconduct and it is possible to obtain several superconducting phases in a single sample. Researchers are attempting to produce a single phase superconducting material, but to date, secondary defect phases are still present.[52,53,54,55] CuO and Bi- and Sr-doped Ca_2CuO_3 insulating phases are the most commonly present defect phases.[55,56,57] These secondary phases act as insulating phases disrupting the continuity of the superconducting phase and greatly hinder the superconductor's ability to transport electricity with no resistance.

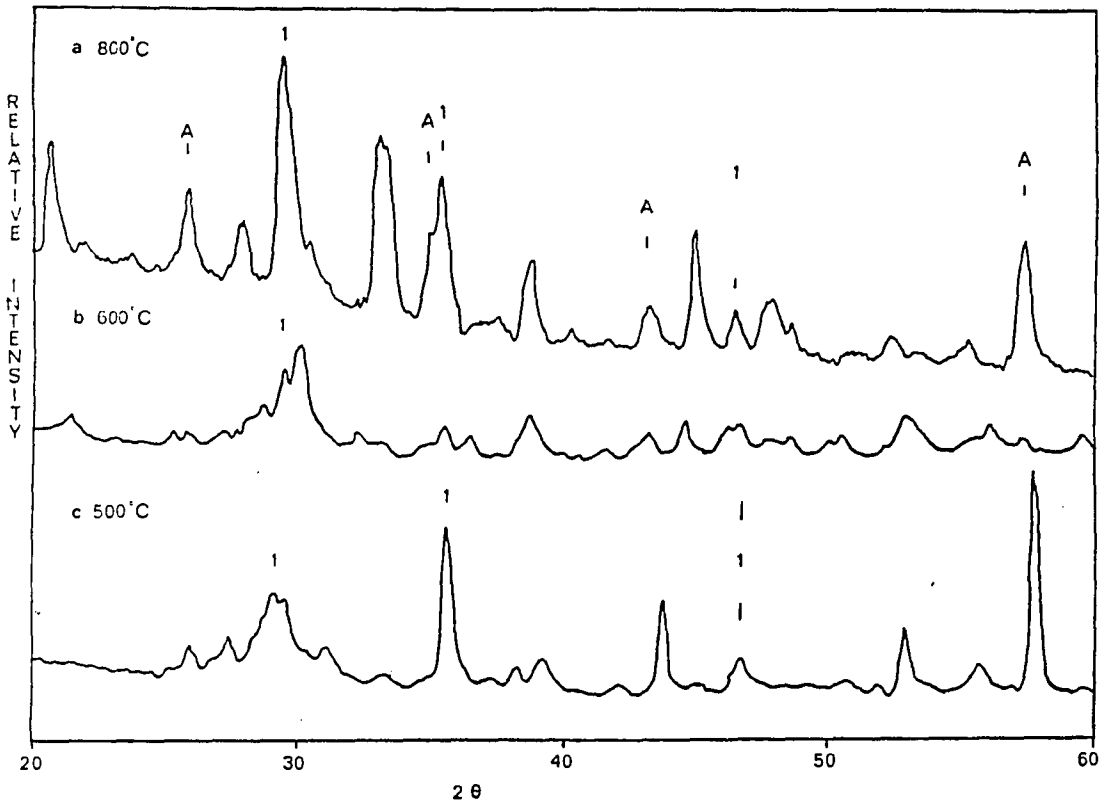

FIGURE 27: XRD traces of films heat treated at (a) 800°C, (b) 600°C, and (c) 500°C in flowing oxygen for 1.5 hours. "A" represents the peaks attributed to the Al_2O_3 substrate and the "1" indicates peaks attributed to the $Bi_4Sr_3Ca_3Cu_4O_{16+x}$ superconducting phase.

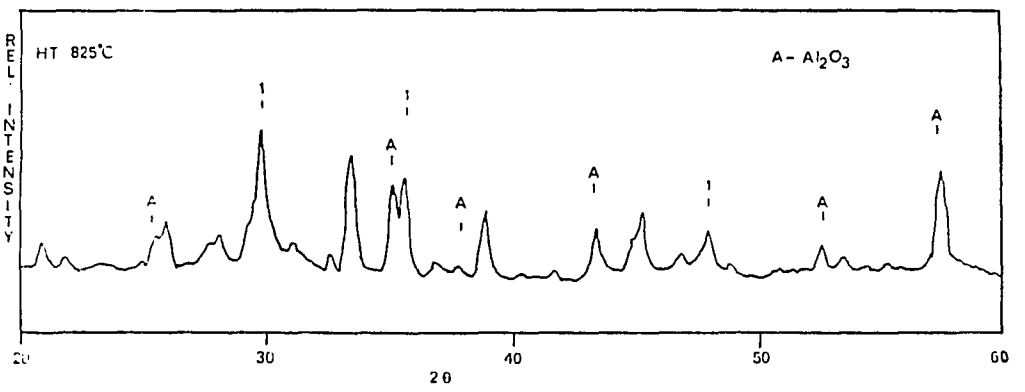

FIGURE 28: XRD trace of a SPP film produced on an Al_2O_3 substrate, heat treated at 825°C for 1.5 hours in flowing oxygen. The superconducting phase is represented by a "1".

SPP films prepared in this study, that were heat treated in flowing oxygen at 825°C for 1.5 hours, showed a single superconducting phase identified by XRD as the $Bi_4Sr_3Ca_3Cu_4O_{16+x}$ phase (Figure 28), which is known to superconduct at $T_c \geq 75$ K.[58] It also contained two secondary phases, identified as BiO and $CuBi_2O_4$ (Table IX). There were also indications that secondary calcium and strontium phases were present in very minute quantities in these films, but due to peak overlapping it was difficult to ascertain exactly what phases were present. An explanation for the lack of secondary calcium and strontium phases in the heat treated films is due to the calcium and strontium phases being completely sacrificed when the superconducting phase is produced. The excess bismuth and copper remaining, form BiO and $CuBi_2O_4$ phases, which produce insulating phases. Therefore the minimization of these phases is desirable, since the insulating properties of these phases hinder the ability to perform resistivity measurements. However, despite the presence of these insulating phases, resistivity measurements were attempted, in an attempt to provide more information on this new $Bi_4Sr_3Ca_3Cu_4O_{16+x}$ superconducting phase. But there was not a continuous superconducting path present, so accurate measurements were not obtained. Meissner effect

TABLE IX: d-spacings from SPP prepared film.

d-spacing (Å)	Phase identification
4.2467	$CuBi_2O_4$
4.0550	Unidentified
3.7893	Unidentified
3.4371	Unidentified
3.2291	BiO
3.1728	BiO
2.9955	$Bi_4Sr_3Ca_3Cu_4O_{16+x}$
2.8732	Unidentified
2.7526	BiO
2.6882	$CuBi_2O_4$
2.5197	$Bi_4Sr_3Ca_3Cu_4O_{16+x}$
2.4338	$CuBi_2O_4$
2.0170	Unidentified
2.0043	Unidentified
1.9395	$CuBi_2O_4$
1.8974	$Bi_4Sr_3Ca_3Cu_4O_{16+x}$
1.8645	Unidentified
1.7113	Unidentified
1.5221	$Bi_4Sr_3Ca_3Cu_4O_{16+x}$

measurements were also attempted, by scraping off the film and measuring its magnetic susceptibility, however the volume of sample produced from the film was not large enough to provide accurate measurements.

The heat treated films were also examined by SEM, to provide information on the surface morphology and further phase identification. Figure 29 reveals the plate-like structure of these films, this has been shown to be the prevailing structure of the Bi-Sr-Ca-Cu-O superconducting phases.[55,57,59,60,61] However the matrix from which the plates are protruding from was identified as the BiO and $CuBi_2O_4$ phases.

Several of the samples heat treated at 825°C for 1.5 hours in flowing oxygen produced a color gradient across the film, as seen Figure 30. This was due to compositional variations in the film, due to the stationary spray nozzle. Examining the aerodynamics of the spray nozzle (Figure 31) reveals how the variations in composition are produced.[62] In region C, the low velocity droplets stray from the main vortex of the aerosol envelope and produce an inhomogeneous film on the outer edges of the films. The black area at the bottom of this film was identified as containing the

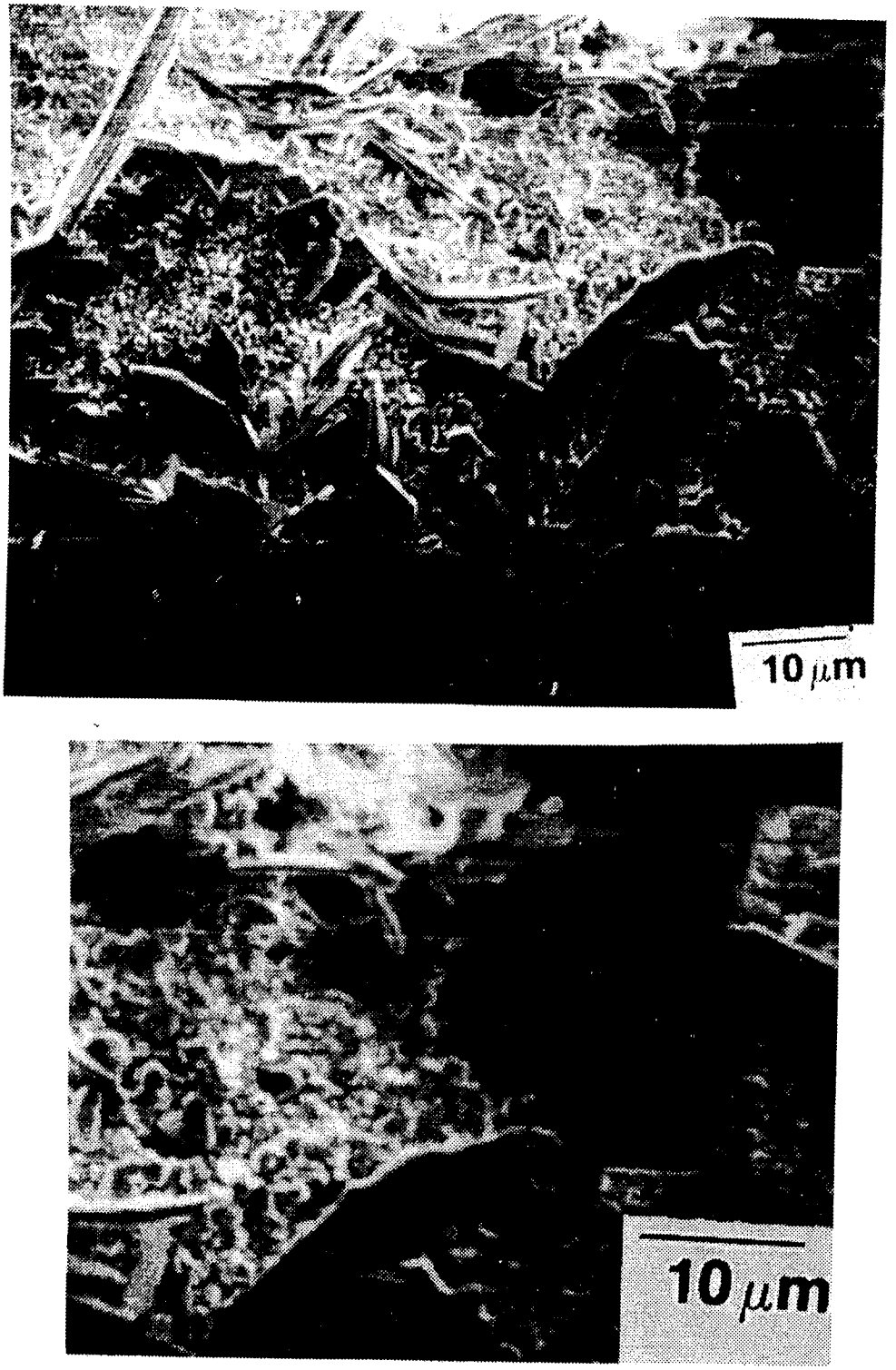

FIGURE 29: SEM photomicrograph showing the plate-like structure developed during heat treatment of Bi-Sr-Ca-Cu-O thin films.

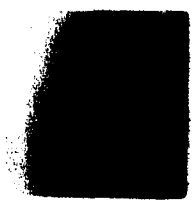

Heat treated 825°C

FIGURE 30: Bi-Sr-Ca-Cu-O thin films produced by SPP and heat treated for 1.5 hours at 825°C. Note the color gradient which represents a compositional variation across the film.

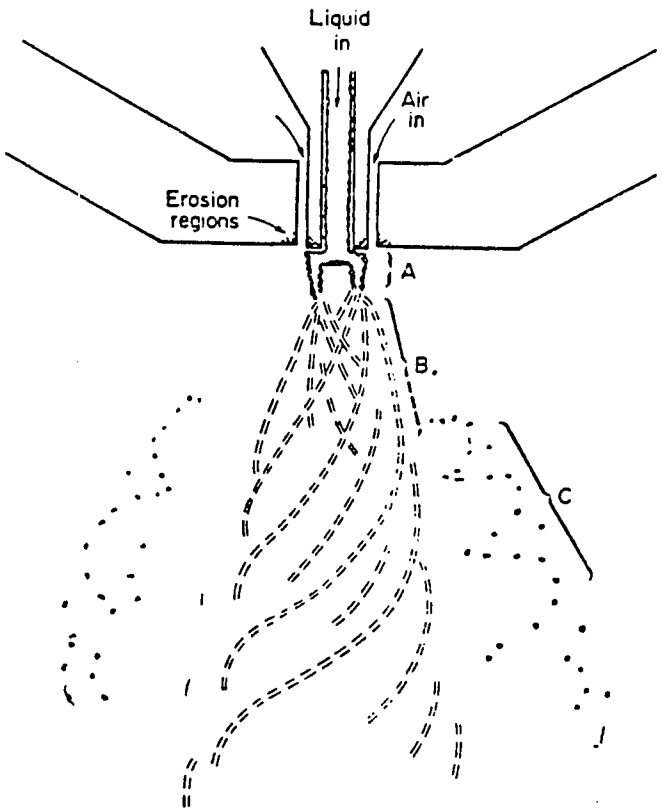

FIGURE 31: Spray envelope for a typical SPP spray nozzle.

$Bi_4Sr_3Ca_3Cu_4O_{16+x}$ phase, while the silvery metallic area contained the pure metals of Bi, Ca, and Sr and, the green area has not been identified, but appears to be a copper oxide phase. Meissner effect measurements were attempted on this sample; however the volume of the superconducting phase was not large enough to obtain accurate measurements. This compositional gradient would suggest that a movable substrate or spray nozzle would be needed if a consistent film composition is desired on a large scale.

CONCLUSIONS

Y-Ba-Cu-O system

1) Y-Ba-Cu-O thin films have successfully been prepared by spray pyrolysis processing from nitrate solutions.

2) Heat treated films showed a close match to the desired 1:2:3 superconducting phase.

Bi-Sr-Ca-Cu-O system

3) Films were successfully prepared by spray pyrolysis using a nitrate/acetate solution.

4) Films sprayed at temperatures >300°C produced black/tan films suggesting the possibility of superconducting phases being present.

5) Films heat treated at 825°C for 1.5 hours produced a close match to the $Bi_4Sr_3Ca_4Cu_3O_{16+x}$ superconducting phase.

APPENDIX I

Superconducting Elements and their superconducting transistion temperatures.

Element	T_c (Kelvin)
Al	1.75 ± 0.002
Be	0.026
Cd	0.517 ± 0.002
Ga	1.083 ± 0.001
Ga(β)	5.9, 6.2
Ga(γ)	7
Ga(Δ)	7.85
Hf	0.128
Hg(α)	4.154 ± 0.001
Hg(β)	3.949
In	3.408 ± 0.001
Ir	0.1125 ± 0.001
La(α)	4.88 ± 0.02
La(β)	6.00 ± 0.1
Lu	0.1 ± 0.03
Mo	0.915 ± 0.005
Nb	9.25 ± 0.02
Os	0.66 ± 0.03
Pa	1.4
Pb	7.196 ± 0.006
Re	1.697 ± 0.006
Ru	0.49 ± 0.015
Sn	3.722 ± 0.001
Ta	4.47 ± 0.04
Tc	7.8 ± 0.1
Th	1.38 ± 0.02
Ti	0.40 ± 0.04
Tl	2.38 ± 0.02
V	5.40 ± 0.05
W	0.00154 ± 0.00005
Zn	0.85 ± 0.01
Zr	0.61 ± 0.15
Zr(ω)	0.65, 0.95

APPENDIX II

Superconducting Compounds Versus Date Discovered

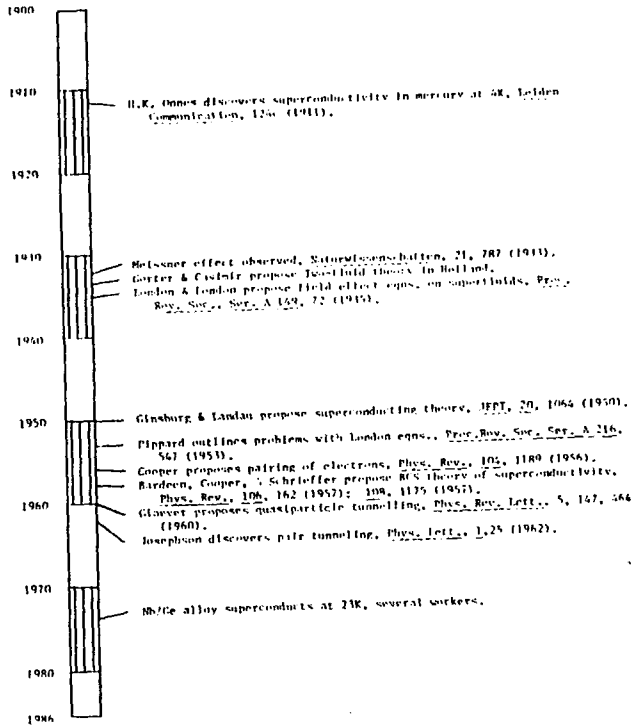

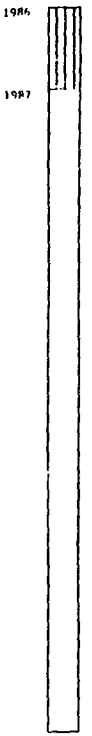

Bednorz & Muller make Ba-La-Cu-O Superconductor at 35K, Z. Phys., B64, 189 (1986).

Others continue work on Ba-La-Cu-O superconductors:
Uchida, Takagi, Kitazawa, Tanaka, Jpn. J. Appl. Phys., Part 2, 2., L1SI (1987).
Takagi, Uchida, Kitazawa, Tanaka, Jpn. J. Appl. Phys., Part 2, 26, L123 (1987).
Jorgensen, Schuttler, Hinks, Capone, Zhang, Brodsky, Scalapino, Phys. Rev. Lett., 58(10), 1024 (1987).
Bednorz, Takashige, Muller, Europhys. Lett., 3(3), 379 (1987).
Chu, Hor, Meng, Gao, Huang, Science, 235(4788), 567 (1987).

Several investigators substitute Ca & Sr for Ba:
Uchida, Takagi, Kitazawa, Tanaka, Jpn. J. Appl. Phys. Lett., 26, L1-L2 (1987).
Ganguly & Rao, Proc. Indian Acad. Sci., Chem. Sci., 97, 831 (1987).
Van Dover, Cava, Battlogg, Rietman, Phys. Rev. B, 35(10), 5337 (1987).
Kanbe, Kishio, Kitazawa, Fueki, Takeuchi, Tanaka, Chem. Lett., 3, 567 (1987).
Bednorz, Muller, & Takashige, Science, 236(4797), 73 (1987).
Tanaka, Jpn. J. Appl. Phys., Part 2, 26(6), L701 (1987).
Tanaka, et. al., Jpn. J. Appl. Phys., Part 2, 26(8), L1136 (1987).
Politis, Geerk, Dietrich, Obst, Z. Phys. B, 66(3), 343 (1987).
Wang, Geiser, Thorn, Douglas, Bowe, Donnelson, Allen, Proksch, Stupka, et. al., Inorg. Chem., 26(8), 1190 (1987).
Cava, van Dover, Batlogg, Rietmann, Phys. Lett., 58(4), 408 (1987).

Several workers investigate Y-Ba-Cu-O superconductors:
Bourne, Cohen, Cooper, Crommie, Stacy, & Zettl, Phys. Lett. A,120, 494 (1987).
Engler, Lee, Nazzal, Beyers, Lim, Grant, Parkin, Ramirez, Vazquez, & Savoy, J. Am. Chem. Soc., 109, 2848 (1987).
Stacy, Radding, Gesselbracht, Wan, Holland, Hoskins, Keller, Millikin, Zur Loye, J. Am. Chem. Soc., 109, 2528 (1987).

A group worked with (Ba-Sr)-La-(Hg-Ag)-Cu-O compounds:
Saito, Noji, Endo, Matsuzaki, Katsumata, Jpn. J. Appl. Phys., Part 2, 26, L223 (1987).

Another group synthesized & characterized Ba-Ba-Cu-O superconductor:
Leigh, Porter, Thorn, Geiser, Owczarek, Wang, Kwok, Kao, Monaghan, Crabtree, Carlson, Williams, Inorg. Chem., 26, 1645 (1987).

Organic superconductivity was investigated:
Tachibana, Inoue, Fueno, Yamabe, & Mori, Synth. Met., 19, 99 (1987).

APPENDIX III

List of Chemical Suppliers

Barium

Nitrate	Strem Chemicals, Inc. Newburyport, MA 01950
$Ba(NO_3)_2$	Alfa Products Morton Thiokol/Ventron Div. 152 Andover St. Danvers, MA 01923

Bismuth

Bi_2O_3	Alfa Products Morton Thiokol/Ventron Div. 152 Andover St. Danvers, MA 01923
$Bi(NO_3)_2$	Alfa Products Morton Thiokol/Ventron Div. 152 Andover St. Danvers, MA 01923

Calcium

$Ca(NO_3)_2$-$4H_2O$	Mallinckrodt, Inc. Paris, Kentucky 40361
CaO	Matheson, Coleman & Bell Norwood, Ohio 45212

Copper

$Cu(NO_3)_2$-$3H_2O$	Alfa Products Morton Thiokol/Ventron Div. 152 Andover St. Danvers, MA 01923
CuO	J.T. Baker Chemical Co. Phillipsburg, N.J. 08885

Cu powder	Alfa Products Morton Thiokol/Ventron Div. 152 Andover St. Danvers, MA 01923

Strontium

$Sr(NO_3)_2$	Alfa Products Morton Thiokol/Ventron Div. 152 Andover St. Danvers, MA 01923

Yttrium

$Y(NO_3)_2$-$5H_2O$	Mallinckrodt, Inc. Paris, Kentucky 40361

APPENDIX IV

Eh-pH diagrams of Ba, Bi, Ca, Cu, Sr, Y

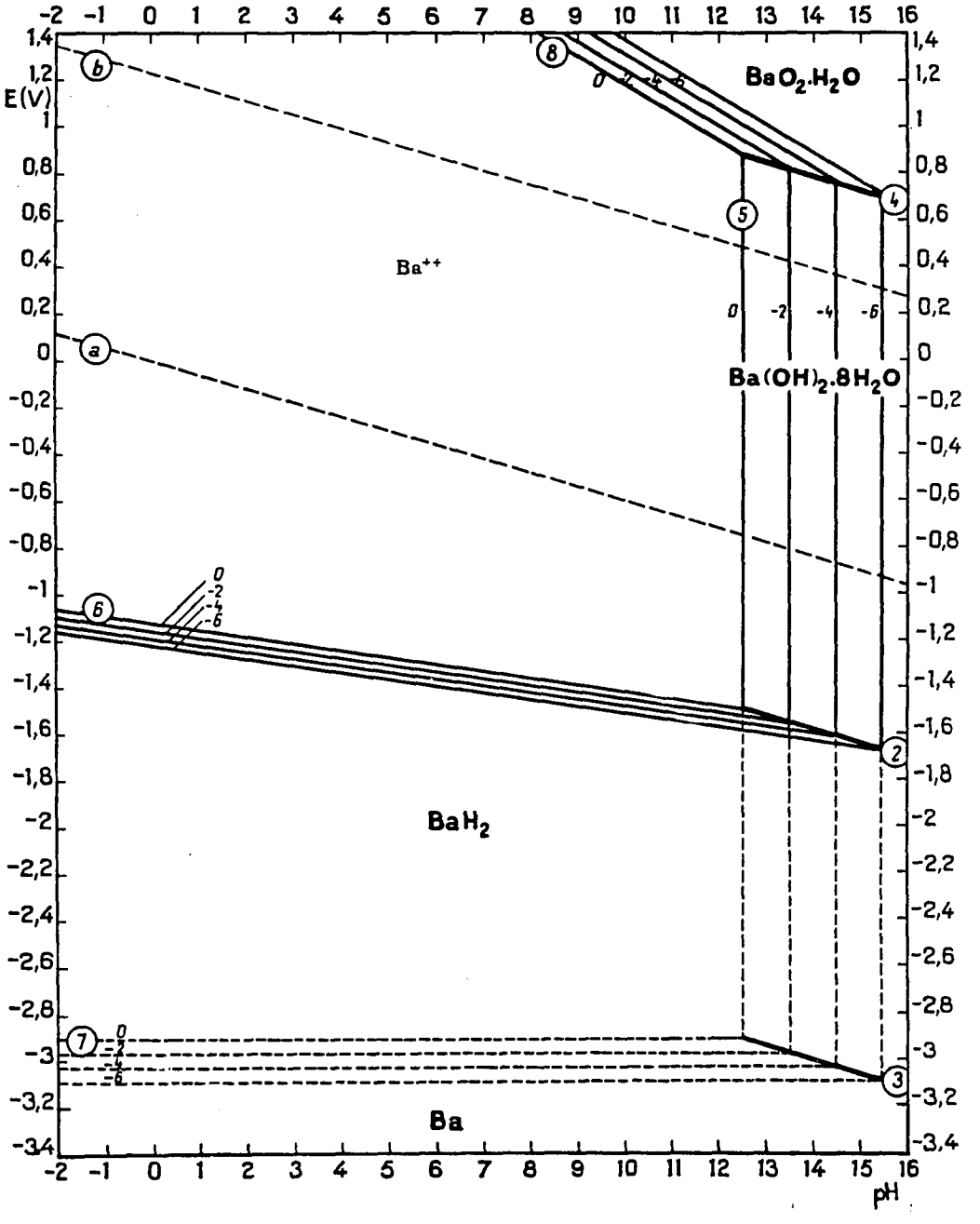

FIGURE 1: Eh-pH diagram of barium-water system at 25°C.

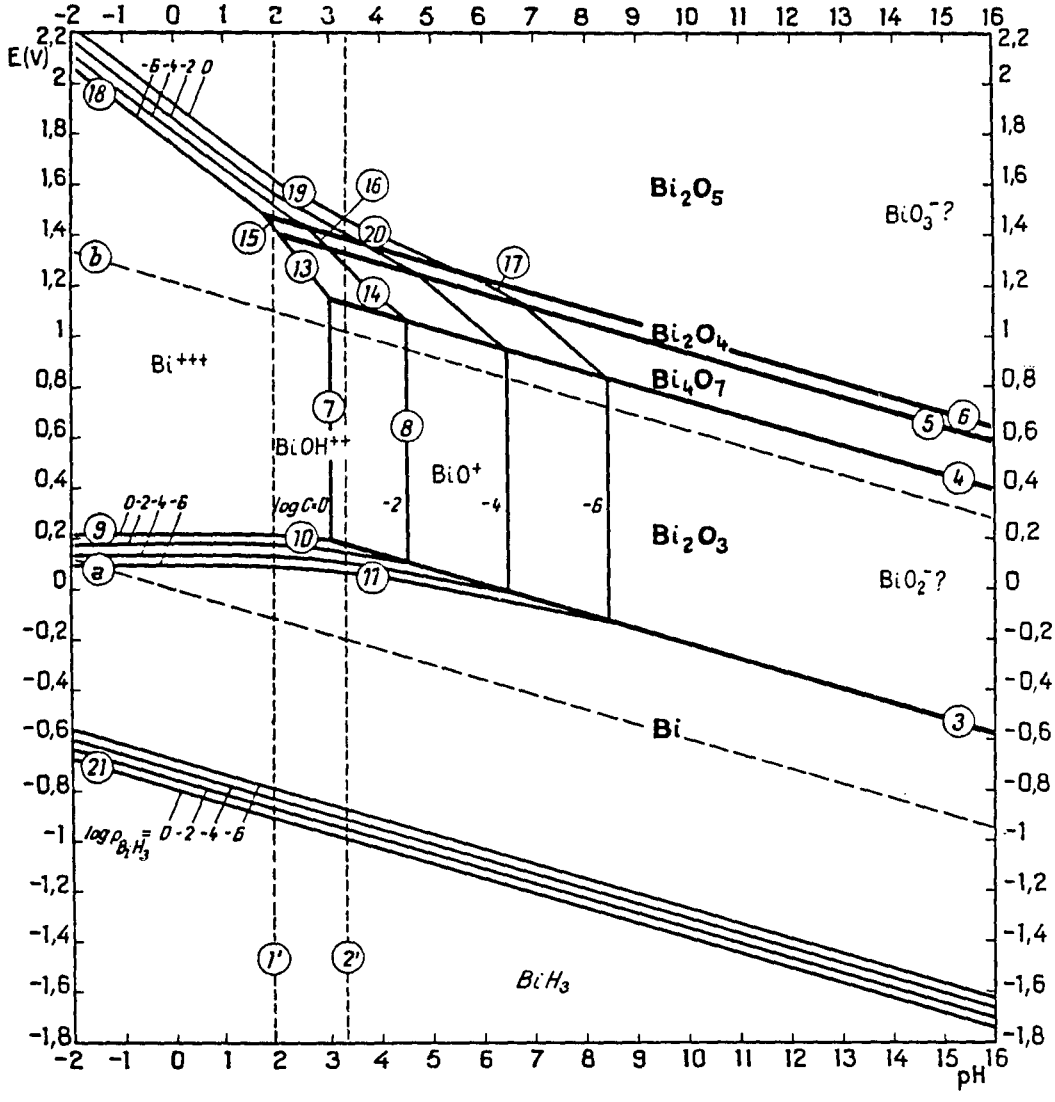

FIGURE 2: Eh-pH diagram of bismuth-water system at 25°C.

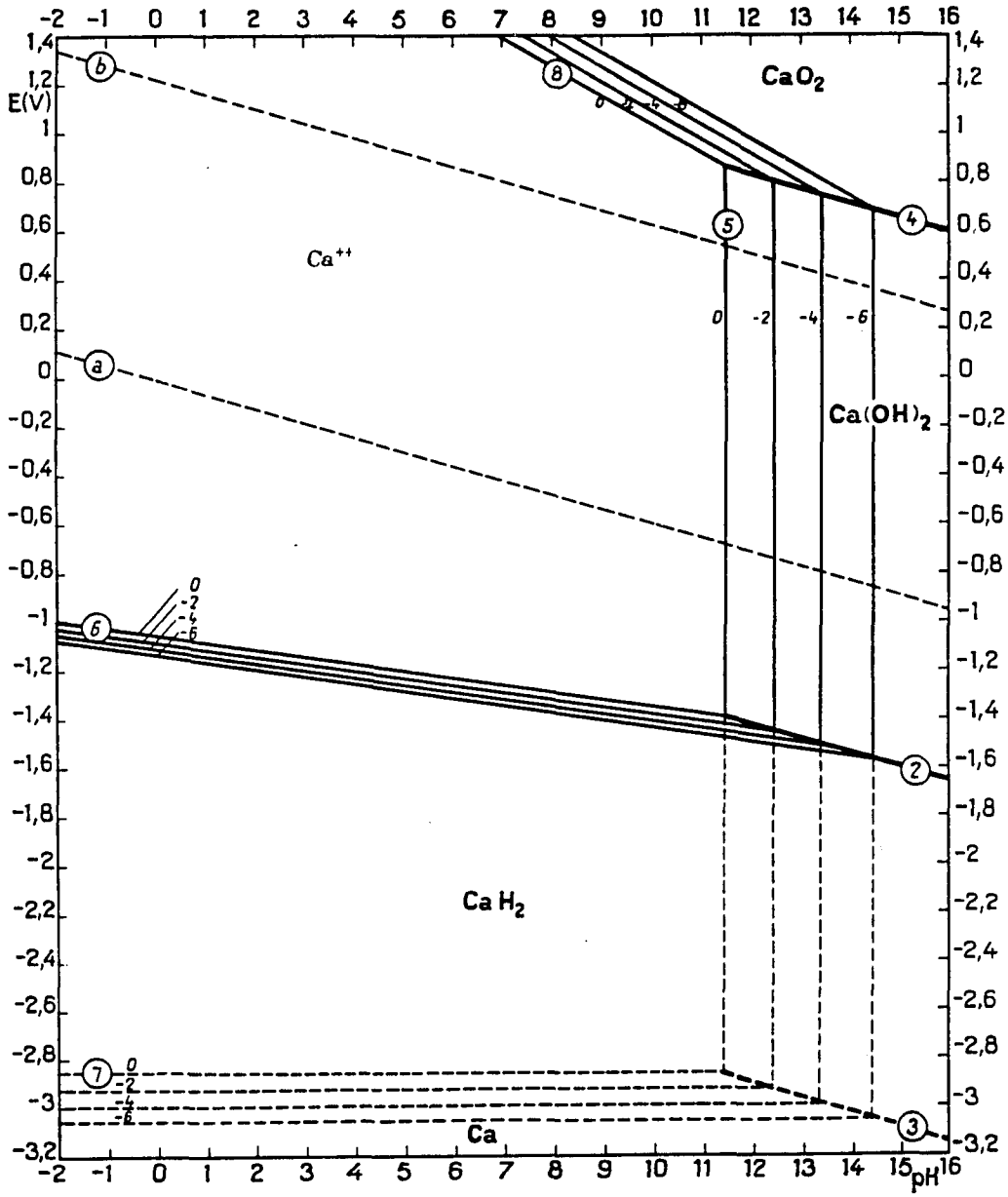

FIGURE 3: Eh-pH diagram of calcium-water system at 25°C.

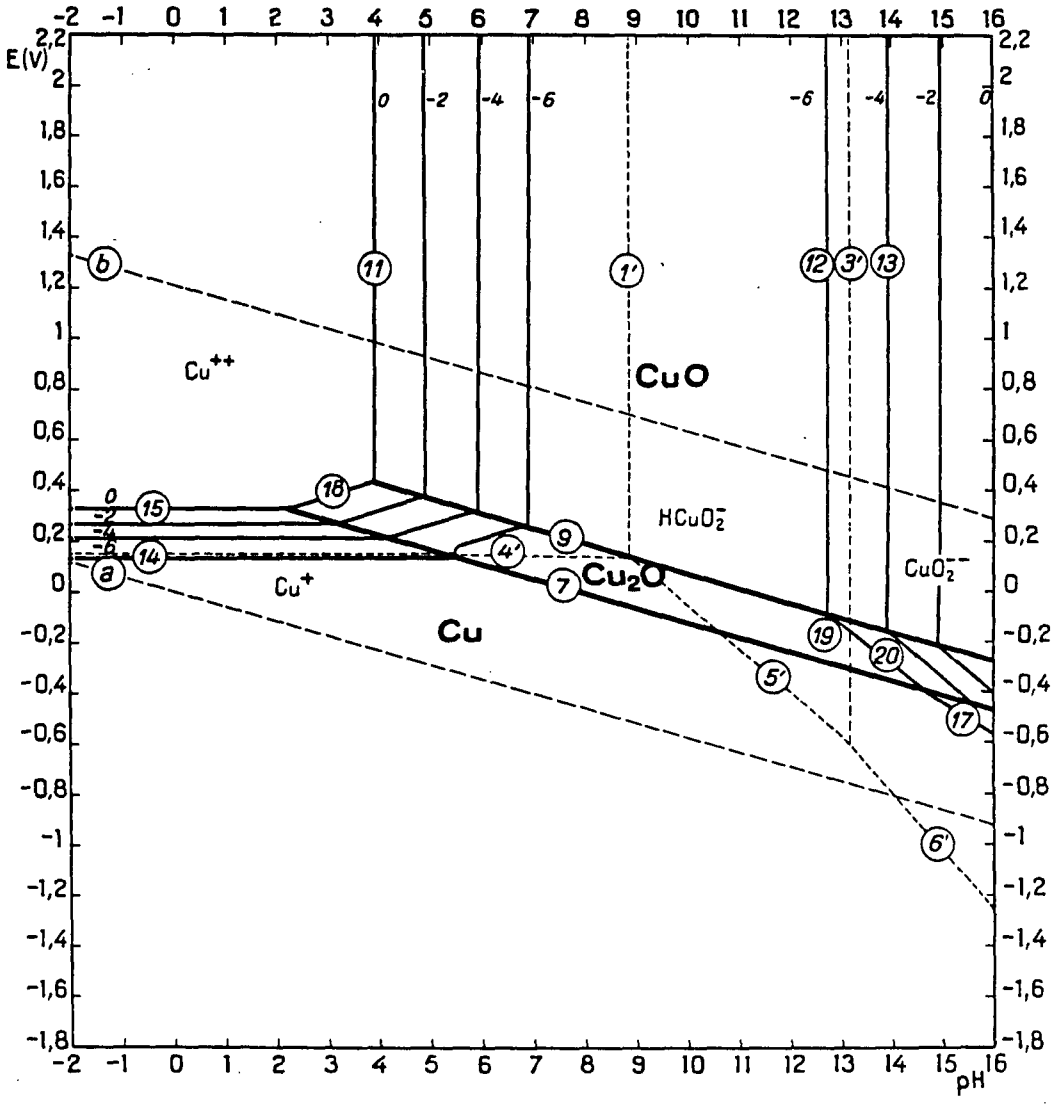

FIGURE 4: Eh-pH diagram of copper-water system at 25°C.

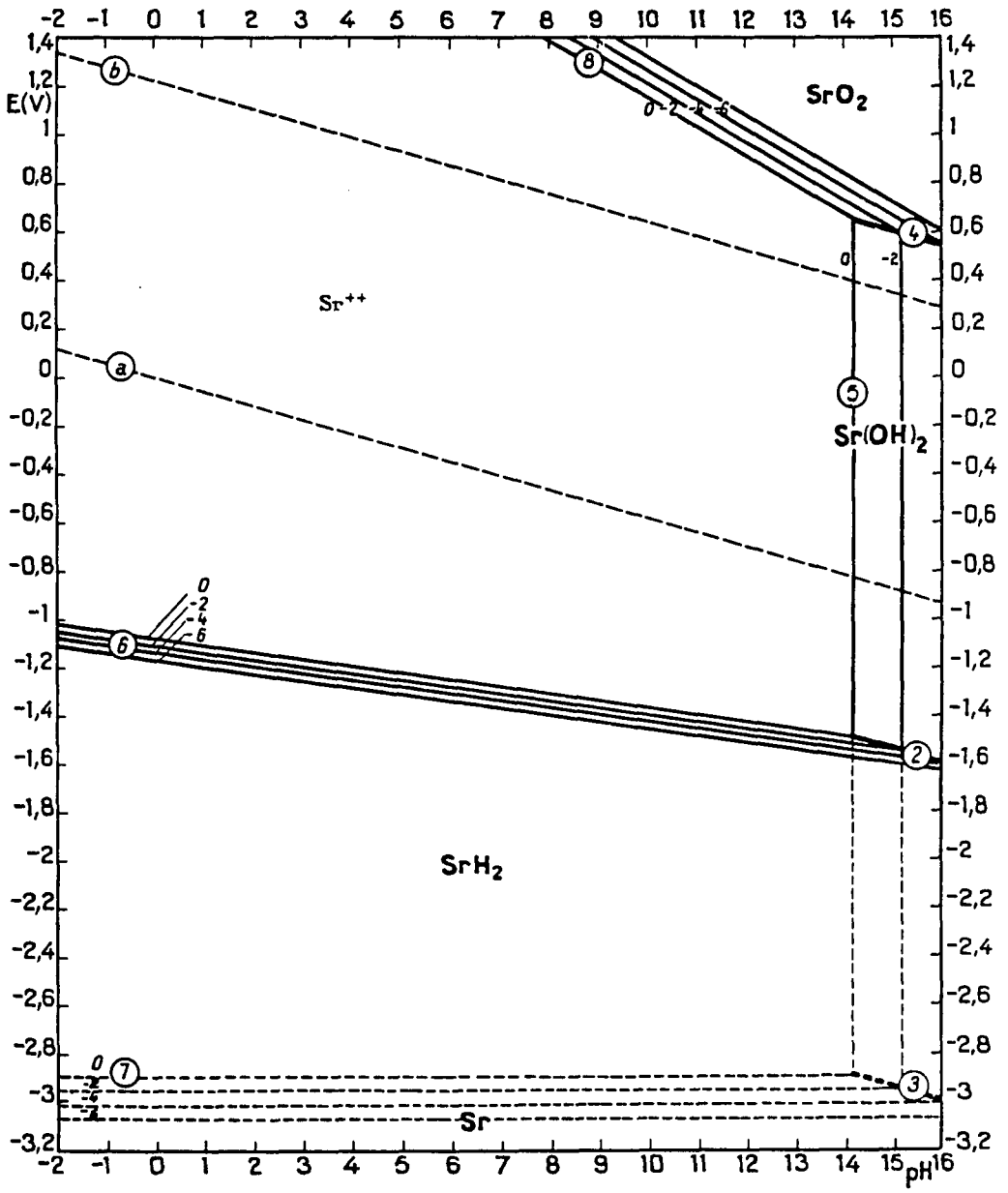

FIGURE 5: Eh-pH diagram of strontium-water at 25°C.

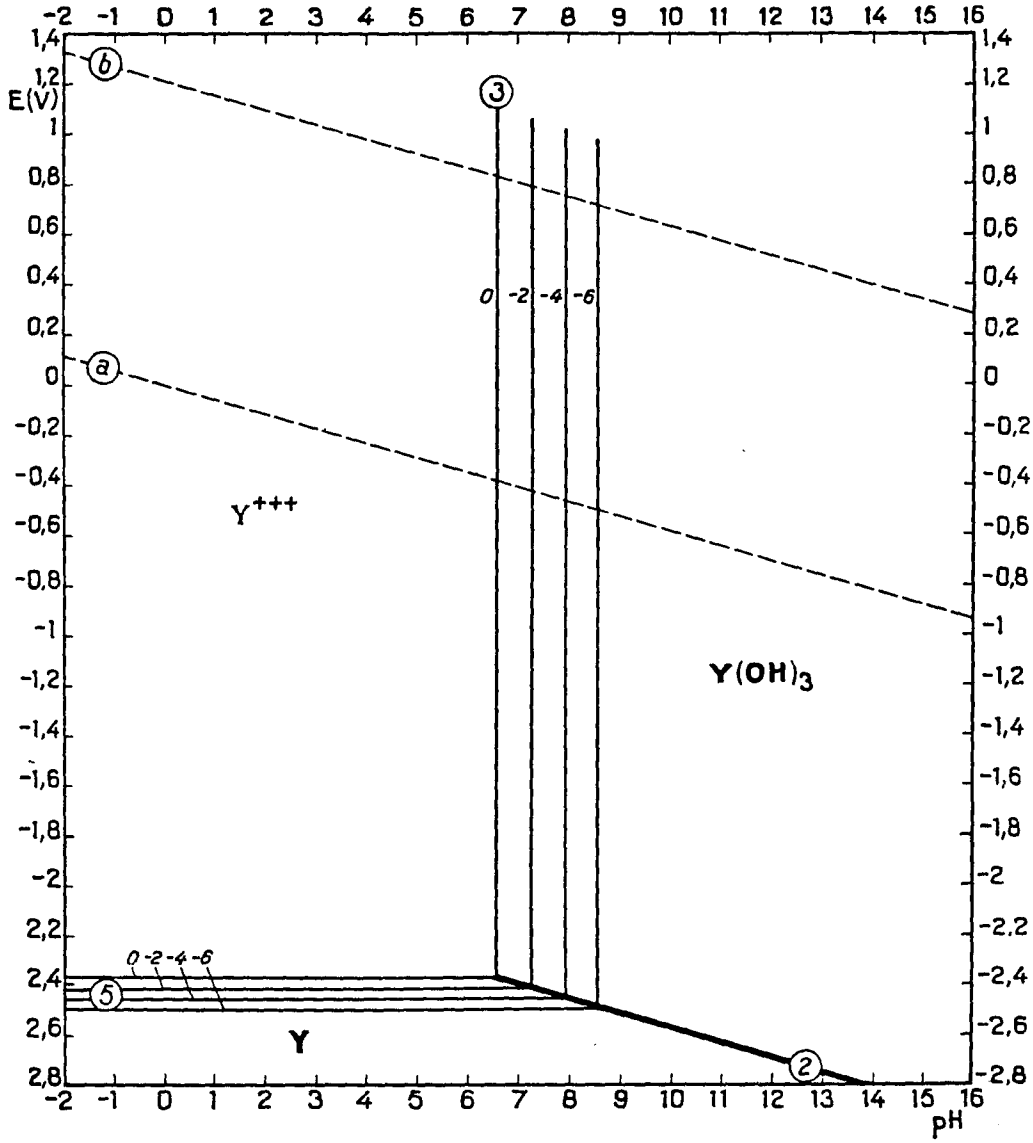

FIGURE 6: Eh-pH diagram of yttrium-water at 25°C.

REFERENCES

1. J.G. Bednorz and K.A. Muller, "Possible High T_c Superconductivity in the Ba-La-Cu-O System," Z. Phys. B-Condensed Matter 64, pp. 189-193 (1986).

2. S.R. Scholes, "Modern Glass Practice," Cahners Books, (1975).

3. J.M. Mochel, U.S. Pat. 2,564,707; 2,564,987; 2,564,709; 2,564,710; 2,564,708; 2,564,706, 1951.

4. R.R. Chamberlin and J.S. Skarman, J. Electrochem. Soc., 113 (1), pp. 86-89, (1966).

5. M. Kawai, et. al., Jpn. J. Appl. Phys., vol. 26, no. 10, Oct. 1987, pp. L1740-L1742.

6. R.L. Henry and H. Lessoff, "Thin Film Growth of $Y_1Ba_2Cu_3O_7$ From Nitrate Solutions," J. of Crystal Growth 85 (1987) pp. 615-618.

7. D.S. Albin and S.H. Risbud, Advanced Ceramic Materials, vol. 2 No. 3A, (1987) pp. 243-252.

8. J.B. Mooney and S.B. Radding, Am. Rev. Mater. Sci. (1982) 12:81-101.

9. G.A. Roderick, 1980 Proc. Eur. Community Photovoltaic Solar Energy Conf., 3rd, Cannes, pp. 327-34. Dordecht, Holland: Reidel.

10. R. Pommier, C. Gril, and J. Marucchi, Thin Solid Films, 77:91-97 (1981).

11. R. Groth, Phys. Status Solidi 14:69-75 (1966).

12. J.B. Mooney, et. al., 1981. SERI Subcontract XS-9-8104-4, Menlo Park, Calif: SRI Int.

13. C.W. Bates, et. al., "Effect of pH of chalcopyrite $CuInSe_2$ prepared by spray pyrolysis," Appl. Phys. Lett., Vol. 43, No.9, pp. 851-852.

14. Y.Y. Ma and R.H. Bube, "Properties of CdS Films Prepared by Spray Pyrolysis," J. Electrochem. Soc., 124 [9] 1430-35 (1977).

15. G. Blandent, M. Court, and Y. Lagarde, "Thin Layers Deposited by the Pyrosol Process," Thin Solid Films, 77, 81-90 (1981).

16. J.C. Viguie and J. Spitz, "Chemical Vapor Deposition at Low Temperatures," J. Electrochem. Soc., 122 [4] 585-88 (1975).

17. W. Siefert, "Properties of Thin In_2O_3 and SnO_2 Films Prepared by Corona Spray Pyrolysis, and a Discussion of the Spray Pyrolysis Process," Thin Solid Films, 121, 275-82 (1984).

18. P. May, et. al., "Production of superconducting thick films by a spin-on process," Supercond. Sci. Technol. 1 (1988) pp. 1-4.

19. M. Gurvitch and A.T. Fiory, "Preparation and substrate reactions of superconducting Y-Ba-Cu-O films," Appl. Phys. Lett. 51 (13), 28 Sept. 1987 pp. 1032-1034.

20. A. Banerjee, et. al., Proc. 7th Int. Solar Energy Congress, New Delhi (1978); Sun: Mankind's Future Source of Energy, Pergammon, Oxford (1978), p. 675.

21. A. Banerjee, Ph.D. Thesis, Indian Institute of Technology, New Delhi (1978).

22. K.L. Chopra and S.R. Das, Thin Film Solar Cells, (1976) pp. 211-220.

23. R.S. Berg, et. al., J. Vac. Sci. Technol. 15(2): 359-62 (1978).

24. H. Kammerlingh Onnes, Leiden Comm., 120b, 122b, 124c (1911).

25. S. Uchida, H. Takagi, K. Kitazawa, S. Tanaka, Jpn. J. Appl. Phys., Part 2, 26, L151 (1987).

26. C.W. Chu, et. al., Science, 235 (4788), 567 (1987).

27. J.D. Jorgensen, et. al., Phys. Rev. Lett., 58, (10), 1024, (1987).

28. S. Uchida, et. al., Jpn. J. Appl. Phys. Lett., 26, L1-L2 (1987).

29. R.B. Van Dover, et. al., Phys. Rev. B, 35, (10), 5337 (1987).

30. P. Ganguly and C.N.R. Rao, Proc. Indian Acad. Sci., Chem. Sci., 97, 631 (1987).

31. M.K. Wu, et. al., Phys. Rev. Lett., 58, 908 (1987).

32. L.C. Bourne, et. al., Phys. Lett. A., 120, 494 (1987).

33. E.M. Engler, J. Am. Chem. Soc., 109, 2848 (1987).

34. A.M. Stacy, et. al., J. Am. Chem. Soc., 109, 2528 (1987).

35. C.W. Chu, et. al., Phys. Rev. Lett. 60, 941 (1988).

36. R.M. Hazen, et. al. Phys. Rev. B 35, 7238 (1987); Erratum B 36, 3966 (1987).

37. H. Maeda, et. al., Jpn. J. Appl. Phys. 63, 2046 (1988).

38. Z.Z. Sheng, et. al., Phys. Rev. Lett. 60, 937 (1988).

39. Z.Z. Sheng and A.M. Hermann, Nature 332, 55 (1988).

40. Superconductivity News, Vol. 1, Number 8, Feb. 18, 1988, p. 1-2.

41. J. Muller and J.L. Olsen, eds., Physica C, Part I and II (1988).

42. D.E. Cox and A.W. Sleight, Sol. St. Comm. 19, 969 (1976).

43. D.E. Cox and A.W. Sleight, Acta Cryst. B 35, 1 (1979).

44. L.F. Mattheiss, MRS Anaheim Symp. (1987), p. 23.

45. S. Hayashi, et. al., "Growth of $Y_1Ba_2Cu_3O_{9-x}$ Single Crystals from the High Temperature Solution," Jpn. J. of Appl. Phys. Vol. 26, No. 7, July 1987, pp. L1197-L1198.

46. R.F. Cook, et. al., "Fracture toughness measurements of $YBa_2Cu_3O_x$ single crystals," Appl. Phys. Lett. 51 (6), 10 Aug. 1987, pp. 454-456.

47. R.S. Roth, J.R. Dennis, and H.F. McMurdie, eds., Phase Diagram for Ceramists, vol. VI, ACS (1987), p. ix.

48. Y. Gao, et. al., "Reaction and intermixing at metal-superconducting interfaces: $Fe/YBa_2Cu_{6.9}$," Appl. Phys. Lett. 51 (13), 28 Sept. 1987 pp. 1032-1034.

49. S. Witanachchi, et. al., "As-deposited Y-Ba-Cu-O superconducting films on silicon at 400°C," Appl. Phys. Lett. 54 (6), 6 February 1989, pp. 578-580.

50. M. Pourbaix, Atlas of Electrochemical Equilibria in Aqueous Solutions, Nat. Assoc. of Corr. Eng. (1974).

51. J.N. Butler, Ionic Equilibrium A Mathematical Approach, Addison-Wesley (1964) p. 375.

52. Lee, H.G., et. al., "Study of the stabilization of the high T_c phase in a BiSrCaCuO system," Appl. Phys. Lett. 54 (4), 23 January 1989, pp. 391-392.

53. Hsu, H.M., et. al., "Dense Bi-Sr-Ca-Cu-O superconducting films prepared by spray pyrolysis," Appl. Phys. Lett. 54 (10), 6 March 1989, pp. 957-959.

54. Zhang, J., et. al., "Organometallic chemical vapor deposition of high T_c superconducting Bi-Sr-Ca-Cu-O films," Appl. Phys. Lett. 54 (12), 20 March 1989, pp. 1166-1168.

55. Carim, A.H., et. al., "Structure and composition in the superconductive Bi-Sr-Ca-Cu-O system," J. Mater. Res. 3 (6), Nov./Dec. 1988, pp. 1317-1326.

56. Sarkar, A.K., et. al., "The effects of long-term annealing on superconducting properties in the Bi-Sr-Ca-Cu-O system," J. Appl. Phys. 65 (6), 15 March 1989, pp. 2392-2397.

57. Lee, H.G., et. al., "Study on the stabilization of the high T_c phase in a BiSrCaCuO system," Appl. Phys. Lett. 54 (4), 23 January 1989, pp. 391-392.

58. Furcone, S.L. and Chiang, Y.M., "Spin-on $Bi_4Sr_3Ca_3Cu_4O_{16+x}$ superconducting thin films from citrate precursors," Appl. Phys. Lett. 52 (25), 20 June 1988, pp. 2180-2183.

59. I. Maartense et. al., "The effects of long-term annealing on superconducting properties in the Bi-Sr-Ca-Cu-O system," J. Appl. Phys. 65(6), 15 March 1989, pp. 2392-2397.

60. T. Nakamori et. al., "Preparation of Superconducting Bi-Ca-Sr-Cu-O Printed Thick Films Using Coprecipitation of Oxalates," Jap. J. Of Appl. Phys. Vol. 27, No. 4, April 1988, pp. L649-L651.

61. A. Perrin et. al., "DC sputtered high-temperature superconducting thin films in the Bi-Sr-Ca-Cu-O system," Supercond. Sci Technol. 1 (1988) pp. 201-204.

62. C.M. Lampkin, "Aerodynamics of Nozzles Used In Spray Pyrolysis," *Prog. Crystal Growth Charact.*, Vol. 1, (1979) pp.405-416.